Patterns of Hemolymph Pressure Related to Tracheal Tube Collapse in the Beetle *Pterostichus commutabulis*

Lewis Michael Cox

Thesis submitted to the faculty of the Virginia Polytechnic Institute and State University
in partial fulfillment of the requirements for the degree of

Master of Science
In
Engineering Mechanics

John J. Socha, Chair
Daniel M. Dudek
Alfred L. Wicks

May 04, 2011
Blacksburg, VA

Keywords: Tracheal tube collapse, insect respiration, hemolymph pressure

Patterns of Hemolymph Pressure Related to Tracheal Tube Collapse in the Beetle *Pterostichus commutabulis*

Lewis Michael Cox

ABSTRACT

Rhythmic collapse and reinflation of tracheal tubes is a form of active ventilation that augments convective gas exchange in multiple orders of insects. The underlying mechanism driving this phenomenon is not known. Among other things, tracheal tube collapse could be caused by either direct impingement of trachea or by a difference of pressure gradients between the intra-tracheal air and the surrounding hemolymph. To determine the relationship between hemolymph pressure and tracheal tube collapse in the ground beetle (*Pterostichus commutabulis)*, we performed direct measurements of hemolymph pressure inside the beetle's prothorax while simultaneously using synchrotron phase contrast imaging to observe morphological changes in the trachea. We observed that a pressure pulse co-occurred with every tube compression observed throughout the body, suggesting that pulses in hemolymph pressure are responsible for tracheal collapse. To assess the effects of the experimental x-ray conditions imposed on the subjects during imaging, hemolymph pressure was also directly measured in the prothorax of beetles less restricted in non-x-ray trials. To compare the pressure patterns in the two experiments, a novel method of identifying and analyzing pressure pulses was developed and applied to the data sets. The comparison provides the first quantitative characterization of a directly measured hemolymph pressure environment, and demonstrates strong similarities in the pressure patterns recorded in both tests. However, pulses occurring during the x-ray experiments exhibited larger average magnitudes. Further video analysis however shows that collapse of the primary tracheal tubes was observed to occur even in the presence of the smallest simultaneously measured pressure pulse (1.01 kPa), suggesting that collapse of the primary tracheal tubes.

Acknowledgements

I would first like to thank the members of my committee for their patience, help, and advice throughout this study.

My advisor, Dr. Jake Socha, for his continual help, advice, and supply of coffee and espresso. Thank you for the opportunity to step out of my comfort zone and immerse myself in interdisciplinary studies.

The other members of the EFRI group for their insightful feedback and suggestions.

Sara Bonham Dellinger for all her time saving advice and continuous reminders of important deadlines.

Elan Dalton for his help with animal care and assistance in running experiments at Argonne National Lab.

Hodjat Pendar for his help with animal care and the video and sound editing he has performed.

Sam Hochgraf for helping with the video analysis.

And finally, I would like to thank all of my friends and family for helping me to keep a healthy perspective on life.

Table of Contents

List of Figures

List of Tables

Chapter 1 - Introduction

The insect tracheal system consists of a complex network of soft, flexible tubes with diameters on the micron to the hundreds of micron scale. The tracheal system connects to the ambient air through valves known as spiracles and facilitates gas exchange at tissue locations throughout the insect body. Insect respiration involves both diffusion and convection of gases throughout this network of tubes. While some species may transport gases through the tracheal system using diffusion alone [1-3], many insects are known to employ convective mechanisms as well [4]. One form of convective gas exchange that consists of rhythmically collapsing and reinflating tracheal tubes has been identified in multiple insect species, including ground beetles (*Platynus decentis*), carpenter ants (*Camponotus pennsylvanicus*), house crickets (*Achaeta domesticus*), and other insects [5]. In a carabid beetle (*Pterostichus stygicus*), tracheal tube compressions have been observed to occur in every body segment, including the legs [6]. Socha et al.[6] found that tracheal tube collapse appeared to occur synchronously in the body, but that not all tubes exhibited the collapsing behavior. Amongst the tubes that were observed to collapse, the depth of collapse was variable along the length of a given tube, and some portions of the tube would remain inflated. Four phases of tube collapse were observed; a region of rapidly decreasing tube diameter was followed by a period of static tube compression; the static compression was succeeded by a rapid increase in tube diameter that led into a period of inter-compression, where tubes maintained their maximum diameter.

The mechanism driving the collapse and reinflation of tracheal tubes is not known. One possible mechanism is physical impingement of the tubes. Tracheal tubes span the animal's body, frequently located near muscular tissues. Muscular contractions throughout the insect could potentially cause tracheal compressions in certain tubes by imposing local stresses on the tube walls. Alternatively, compression could arise from a hydrostatic pressure difference forming across the tube wall. Hemolymph (insect blood) is found throughout the body cavities of insects, surrounding tracheal tubes and other

anatomical structures. Differences between the intra-tracheal and hemolymph pressures impose either expansive or compressive forces on the tracheal tubes. If the compressive pressure diference were to become sufficiently large it could induce tube collapse. Changes in the pressure gradient across the tube wall could arise due to fluctuations in the intra-tracheal pressure, the hemolymph pressure, or a combination of both.

The behavior of intra-tracheal pressures in insect respiration has been subjected to some investigation. When the insect's spiracles are opened to the air, intra-tracheal pressure immediately inside of the spiracles assumes an atmospheric magnitude [7, 8]. Sub-atmospheric intra-tracheal pressures may also occur due to passive diffusion when the spiracles are closed; closed spiracles can cause pressure gradients to form as oxygen becomes depleted inside the tracheal tubes [9]. Intra-tracheal pressures were measured to tend towards atmospheric pressure, but exhibited jumps both above and below this level in the dung beetle, *Circellium bacchus* [10]. It is possible that the sub-ambient pressures in the tracheal tubes could either cause or augment tube collapse. Sub-atmospheric tube pressures could also arise from decreasing hemolymph pressures, which, during periods where spiracles are closed, would exert an expansive force on the tubes. This situation, however, would not contribute to tracheal tube collapse, but instead induce expansion.

Increasing hemolymph pressures relative to the intra-tracheal pressure would exert compressive forces on tubes. Fluctuations in hemolymph pressure can be induced via volumetric changes in body segments [11, 12]. Using externally applied strain-gauge transducers to indirectly measure hemolymph pressure in the pupae of some endopterygote insects, rhythmic pressure pulses were inferred to occur synchronously with the contractions of intersegmental abdominal muscles [13]. These pressure pulses were observed to start and terminate at a baseline pressure between 0.5 and 1 kPa below atmospheric levels, but peak magnitudes of these pulses were not reported to exceed atmospheric pressures in the larva. While these pressure fluctuations could cause tracheal deformation, it would be impossible for sub-atmospheric hemolymph pressure pulses to induce collapse of tracheal tubes unless the intra-tracheal pressure were to simultaneously drop to an even larger degree. Direct measurements of hemolymph pressure have been recorded in a tenibrionid beetle (*Zophobas atratus*) that exhibit pulses with peak

amplitudes above atmospheric level (approximately 2.66 kPa) [14]. Such pulsations suggest that it may be possible for hemolymph pressure to achieve magnitudes sufficiently larger than the intra-tracheal pressure and act as the driving mechanism for the rhythmic collapse of tracheal tubes.

In this study, we investigate hemolymph pressure in the broader aim of identifying the physiological mechanism of tracheal tube collapse in one species of carabid beetle (*Pterostichus commutabulis*). We expect to observe pressure pulses above atmospheric levels in the beetles' hemolymph that exhibit rhythmic patterns similar to the patterns of tracheal tube collapse observed in a different species (*Pterostichus stygicus*) by Socha et al. [6]. We address this hypothesis by directly measuring the hemolymph pressure in the prothorax of live beetles. Patterns of pressure are characterized, providing the first description of a directly measured hemolymph pressure environment in a carabid beetle, and are compared to patterns of tube collapse.

If hemolymph pressure pulses are indeed the driving mechanism of tracheal tube collapse in these beetles, every tube collapse should be accompanied by a pressure pulse. Accordingly, we hypothesized that a pulse in hemolymph pressure would accompany every collapse of tracheal tubes. To address this issue, we directly recorded the hemolymph pressure while concurrently imaging beetles with synchrotron x-rays.

To image the tracheal system and observe tube collapse, beetles were constrained and subjected to synchrotron radiation, which is known to have detrimental effects on organisms [15]. To assess if tube collapse is solely a result of the experimental conditions imposed on the beetles during imaging, we compared the hemolymph pressure patterns characterized in the x-ray trials to those from non-x-ray lab trials.

Chapter 2 - Methods

2.1 Animals

Carabid beetles (*Pterostichus commutabulis*) were locally collected using pitfall traps. They were maintained in a terrarium containing a mixture of sand and soil and were provided dog chow and water ad libitum. Seventeen specimens (both male and female, 8 in the box and 9 in the x-ray experiments) were used, with mass 162 +/- 19 mg (mean +/- s.d., hereafter).

2.2 Box Trials

Two fiber optic pressure transducers (Samba Preclin 420 LP Series 200; Vastra Frolunda, Sweden) with a 420 micrometer diameter were used to measure pressures. They were calibrated statically using a water column and have an accuracy of +/- 0.05 kPa. Prior to each trial, ambient pressures were recorded on both sensors. To determine if the hemolymph pressure exhibits patterns of pulses similar to the patterns of previously observed tube collapse, the hemolymph pressure was recorded inside the prothorax of beetles contained in a small box. Beetles were massed, cold anesthetized at ~2^{o}C, and placed on an aluminum block. To avoid damaging the heart and the primary tracheal tubes located along the middle of the prothorax, a hole was drilled into the right-center portion of the prothorax using a 0.5 mm bit. Using a micrometer (THORLABS manual 25 mm translation stage), one pressure transducer was then inserted into the prothorax to a depth of approximately 1 mm. Because the beetles' body would shift during this insertion the depth had to be approximated using a visual landmark on the sensor measured to be 1.1 +/- 0.025 mm along the length of the sensor. The sensor was then sealed using a nail polish adhesive (Sally Hansen Hard as Nails Strengthening Topcoat). After a minimum of 20 minutes for the adhesive to cure, the beetle was moved to an acrylic box (2.5x1.0x0.6 cm, Figure **2.1**). The purpose of the box was to leave the beetle as unconstrained as possible, with sufficient room to move around, but not enough to dislodge the pressure transducer from the seal. Accordingly, the box dimensions were fabricated to allow specimens a small amount of translational movement along three

axes. Due to the adherence of the pressure transducer to the thorax, forces were still imposed on the animals' bodies, providing some constraint. The box contained an optical sensor facing the posterior end of the beetle to monitor movement, while the anterior portion of the box was covered in black tape to provide a darkened environment. A single layer of paper towels was laid across the bottom of the chamber to provide traction. The second fiber optic pressure transducer was affixed near the box to record ambient pressure.

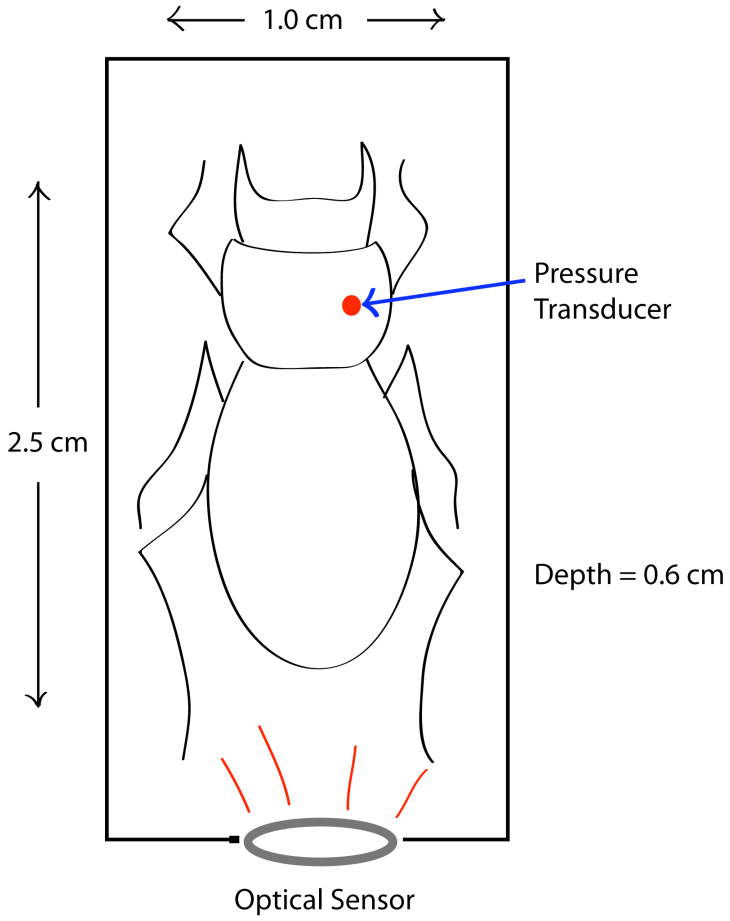

Figure 2.1: Beetles sealed in a box. Dimensions were chosen such that the box was larger than the bodies of the beetles but still limited the range of motion to prevent the pressure transducer from dislodging. Not shown is the box lid with a notch that extends the length of the beetle, allowing the pressure transducer to translate with the animal.

At the beginning and end of each trial the temperature (23.8 +/- 0.9 ^{o}C) and relative humidity (40 +/- 4%) of the room were recorded. With the lid sealed on and the

beetle secured in the box, data on the hemolymph pressure, ambient pressure, and movement were simultaneously recorded at a 10 Hz sampling rate. A minimum of two hours recording time was required for a trial to be considered successful. If the pressure transducer was dislodged before this point, trials were not considered for analysis. Furthermore, beetles were observed for 24 hours after testing to monitor the animals' condition. If beetles died or behaved irregularly after this period, data was not considered for analysis. A total of 30 trials were attempted. During 19 of these trials the sensor dislodged early, and the specimens used in 3 trials either died (two) or appeared injured (one). A total of 8 trials were considered successful and considered for analysis.

2.3 X-ray Trials

To determine the relationship between thoracic hemolmph pressure and tracheal collapse, a similar set-up was used at Argonne National Laboratory (Argonne, IL, USA). After being cold anesthetized, however, beetles were constrained by surrounding the lateral edges, head, and posterior edges of their body with adhesive putty to minimize their ability to move; beetles were still able to exhibit small movements despite these constraints. Beetles were not constrained along the dorsal and ventral surfaces so that x-rays could pass through the body unobstructed by the putty. Specimens were then positioned dorsal-ventrally in front of the synchrotron beam on a motorized platform capable of translating along two axes (Figure **2.2**). After the beetles were properly positioned, a pressure transducer was inserted and sealed into the prothorax in the same manner as before. A second fiber optic pressure transducer was affixed near the constrained beetle to record ambient pressure.

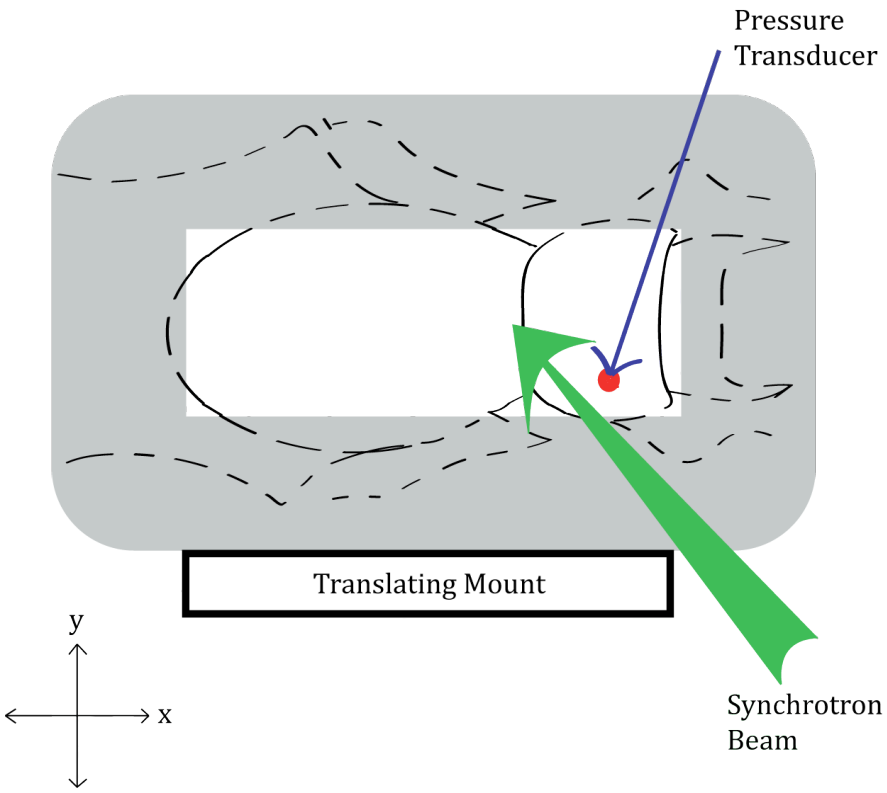

Figure 2.2: Beetle set-up during x-ray trials. Constrained beetles are positioned so that the x-ray beam passes through the dorsal and ventral surfaces. The mount is capable of translating in the horizontal and vertical directions (x, y). Grey area indicates the presence of adhesive putty.

Once the animal was correctly positioned, the temperature (24.01+/- 0.1 ^{o}C) and relative humidity (30.9 +/- 0.6%) were recorded. The hemolymph and ambient pressures were simultaneously recorded at a 10 Hz sampling rate. Pressures were recorded for a minimum of 15 minutes without the presence of x-rays. A voltage pulse was then used to sync the video recording with the pressure measurements and the synchrotron beam was turned on. The maximum temporal uncertainty associated with this technique of synching the pressure and video recordings is 0.1 seconds. In each trial, images were recorded at standard video rates (30Hz) using a video camera (Cohu 4920, Cohu, San Diego, CA, USA) and a 2x microscope objective. The full field of view was 3.2mm X 2.4mm. Movie clips were downloaded to a Macintosh computer using Adobe Premiere

software (Adobe, San Jose, CA, USA). During video recording, the specimens were translated in order to obtain data from all visible portions of their body (i.e. body areas not constrained by putty). Synchrotron x-ray image data were collected at the XOR-32ID undulator beamline at the Advanced Photon Source (Argonne National Laboratory, Argonne, IL, USA). Phase-enhanced images were created using monochromatic x-rays (25keV), a scintillator screen (cerium-doped yttrium aluminum garnet), and a sample-to-scintillator distance of ~0.5m. For more details of this method, see Socha et al. (Socha et al., 2007). A total of 9 trials were performed.

2.4 Analysis

2.4.1 Data Selection

Only certain portions of the trials were analyzed quantitatively. For consistency, we restricted our analyses to a 2 hour window after allowing 30 minutes of recovery from the surgery and cold anesthetizing. Pressure recordings taken during periods of large-scale movement were also excluded from characterization. In the box experiments large-scale movement was defined as any voltage fluctuation recorded by the optical sensor exceeding a 0.2 Volt change in magnitude occurring in a 0.3 second time frame or less. Beetles were observed during experimentation to confirm that voltage oscillations of this magnitude corresponded to periods where the beetle exhibited visible body motions. In the x-ray experiments no optical sensor was used. Despite constraining beetles with putty, periods of movement were also visually identified in the x-ray videos. To characterize patterns of hemolymph pressure, a set of 400 pressure pulses (50 from each trial) from the box experiments and 90 pressure pulses (10 from each trial) from the x-ray experiments were quantified in detail. The longest subsets of pressure recordings uninterrupted by instances of motion were selected for characterization. The difference in the number of pulses characterized is a result of the amount of data available. In order to characterize an equal number of pulses from each animal in the respective experiments, the sample size was determined by the limiting trial. In the x-ray experiment, trial durations were shorter and bodily movements of animals in some trials obscured data much of the data.

2.4.2 Pulse Characterization

In the trials without x-ray visualization of tracheal tubes, large pulses were observed to occur with similar shape regions (Figure 2.3).

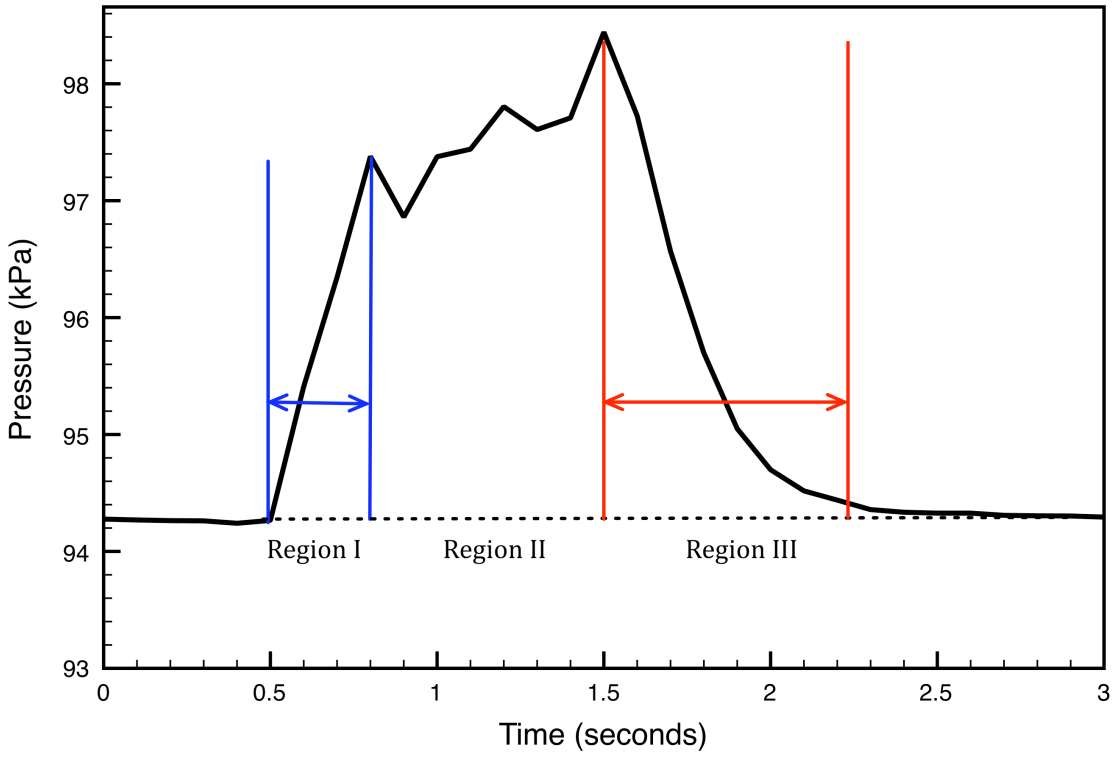

Figure 2.3: Observing three different pulse regions. Region I corresponds to a period rapid pressure rise; Region II is a period of pressure fluctuation; Region III is a period of rapidly decreasing pressure.

To characterize pressure patterns of these larger pulses an algorithm was developed to provide a consistent methodology for comparing pulse parameters, in particular pulse frequency and durations, the durations and rates of change in the different regions, as well as pulse magnitudes. We define a pulse as any rise in pressure larger than a threshold value of 0.5 kPa above the baseline pressure. This threshold value is chosen since it is observed to be the lower limit at which these pulses occur and because the smaller, more erratic fluctuations are consistently seen to remain below it. From here on, pressure patterns occurring below this threshold value will be referred to as secondary fluctuations.

Two measures of pulse magnitude are reported in this study: The peak magnitude relative to the ambient pressure and the peak magnitude relative to the baseline pressure. This algorithm identifies 5 discrete points on each pressure pulse: Start of the pulse, end of the pulse, peak magnitude, and the two points of transition between the pulse regions. The baseline pressure is defined as the average magnitude of hemolymph pressure occurring in between instances of pressure pulses. To calculate this value, the segments of data exhibiting consistent inter-pulse pressures across each data subset were averaged. This value is extrapolated across each data subset and is used to establish a baseline pressure in areas where secondary pressure fluctuations and rapid successions of pulses prevent a consistent baseline from being identified.

Using the values associated with baseline and threshold pressures the raw hemolymph data were passed through a simple algorithm. In Figure 2.4a, raw data recorded from the pressure transducers is shown, with the baseline and threshold pressures superimposed. Three pressure pulses are present in the graph as well as some secondary pressure fluctuations between the second and third pulses. In Figure 2.4b, data existing below the threshold values have been removed. The pressure trace is still shown in blue while the discrete data points are indicated in black. The only exception to the elimination of pressure data below the threshold is a single data point associated with the rise and fall of each pulse. The slope is then calculated by fitting a line to the three data points surrounding the threshold value (one point below it, two above it, Figure 2.4b). The purpose of retaining the sub-threshold data point is to accommodate pulses with magnitudes near the threshold value. In these instances three data points were not always available for a line fit. In Figure **2**.**1**c the slope of the line has been used to extrapolate from the data point immediately above the threshold value, down to the baseline pressure. This process is completed for each pulse resulting in the filtered pressure traces shown in Appendix C.

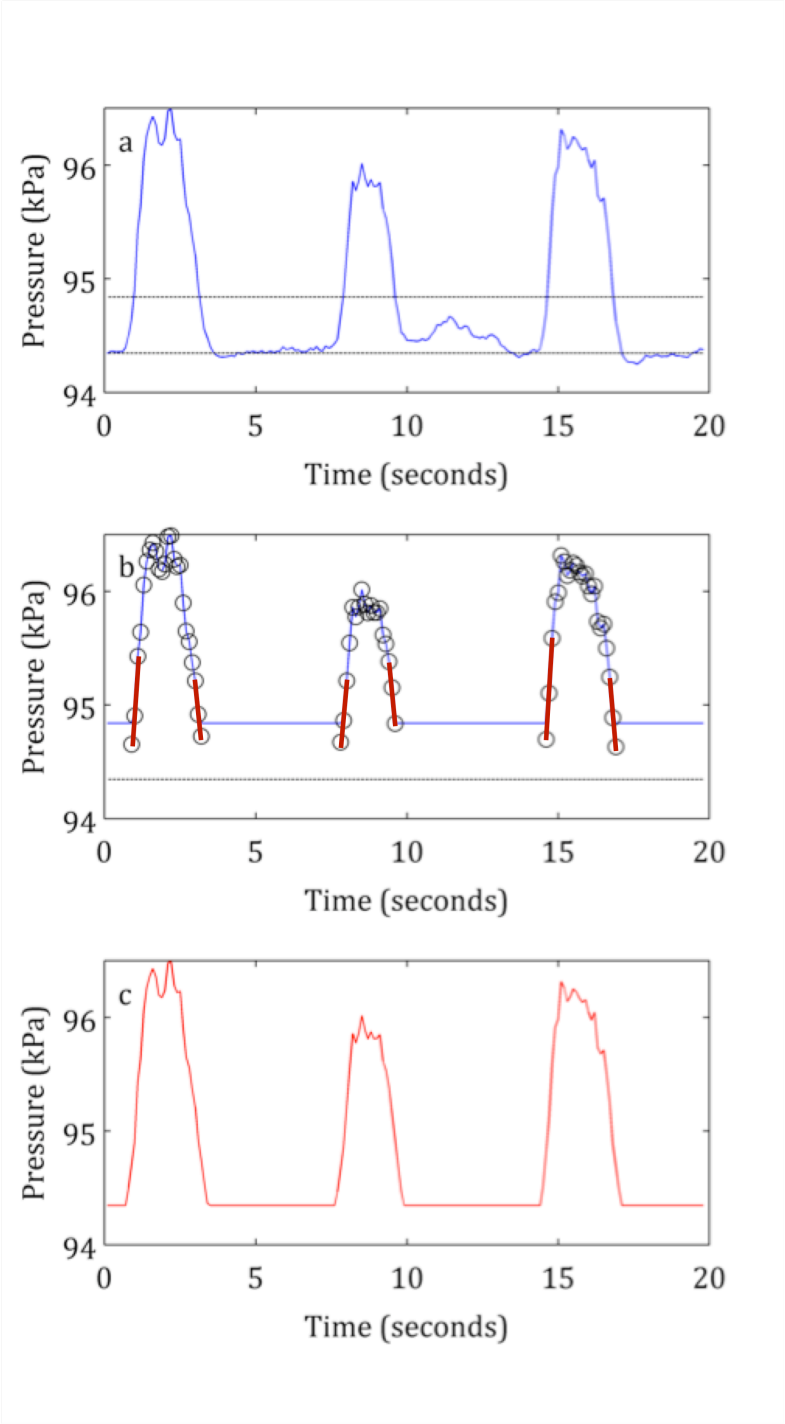

Figure 2.4: Pressure pulse quantification. The baseline and threshold pressures are superimposed on a segment of raw pressure data (a). All raw data below the threshold value is then discarded with the exception of a single data point (discrete data points shown in black) retained below the threshold in Region I and III of each pulse (b). A line is fit to the data points immediately below the threshold and the two adjacent data points above the threshold, shown in red (b). The slope of this line is used to extrapolate from the points immediately above the threshold down to the baseline (c).

In order to identify where each region (Figure 2.3) begins and ends, we defined a windowing algorithm such that its results consistently agree with visually identified patterns. The window spans 0.4 seconds and calculates the average rate of change of the hemolymph pressure within its domain. To identify the point of distinction between Region I and Region II, the window is initially centered on the data point located 0.2 seconds after the start of the pressure pulse. In this manner the rate of change of pressure during the first 0.4 seconds of the pressure pulse is calculated. The window is then incremented by one data point (0.1 seconds) and the rate of change is calculated and compared to the previous value (Figure 2.5). This process continues until the rate of change decreases by 50% from one window increment to the next. The second to last data point to be windowed is then identified as the transition point from Region I to Region II. To identify the point of distinction between Region III and Region II the same process is applied, except the window is initially centered 0.2 seconds before the end of the pressure pulse and is incremented backwards in time (Figure 2.5). The end result of filtering this data through the algorithm is presented in Figure **2**.**6**.

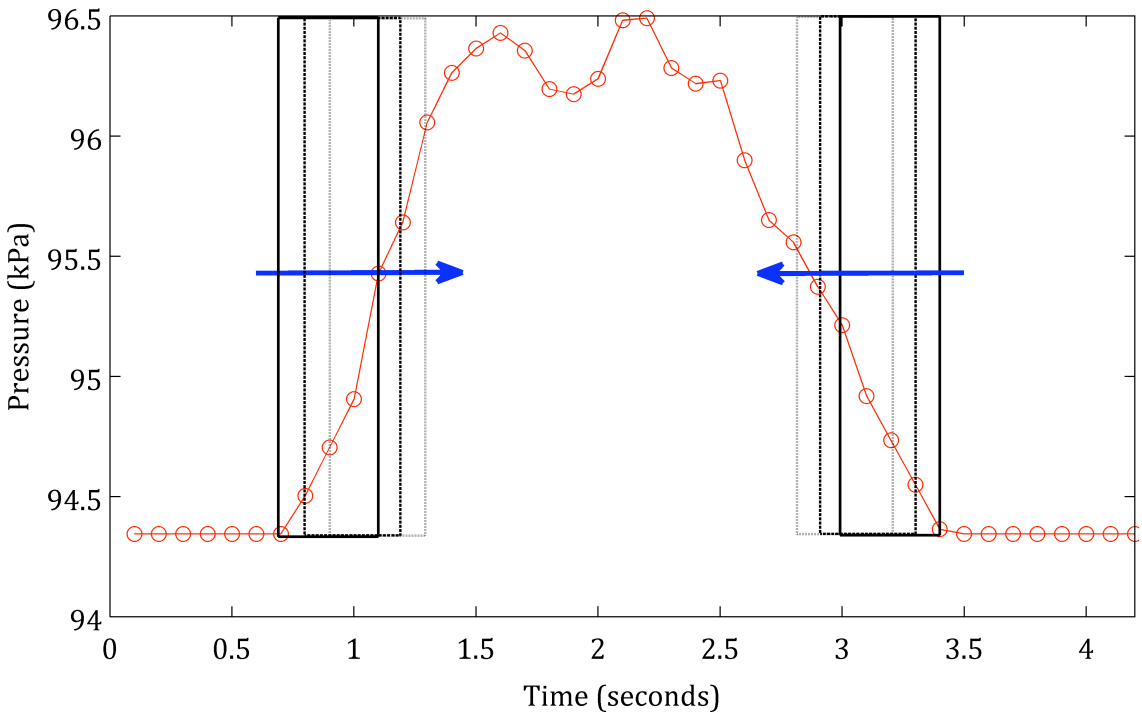

Figure 2.5: A 0.4 second window calculating the average rate of change in pressure is used to identify pulse regions. The window is positioned at the beginning and end points of the pressure pulse than respectively incremented either forward or backward. The data point after which the average rate of change calculated in the next window increment decreases by 50% or more is defined as the transition point.

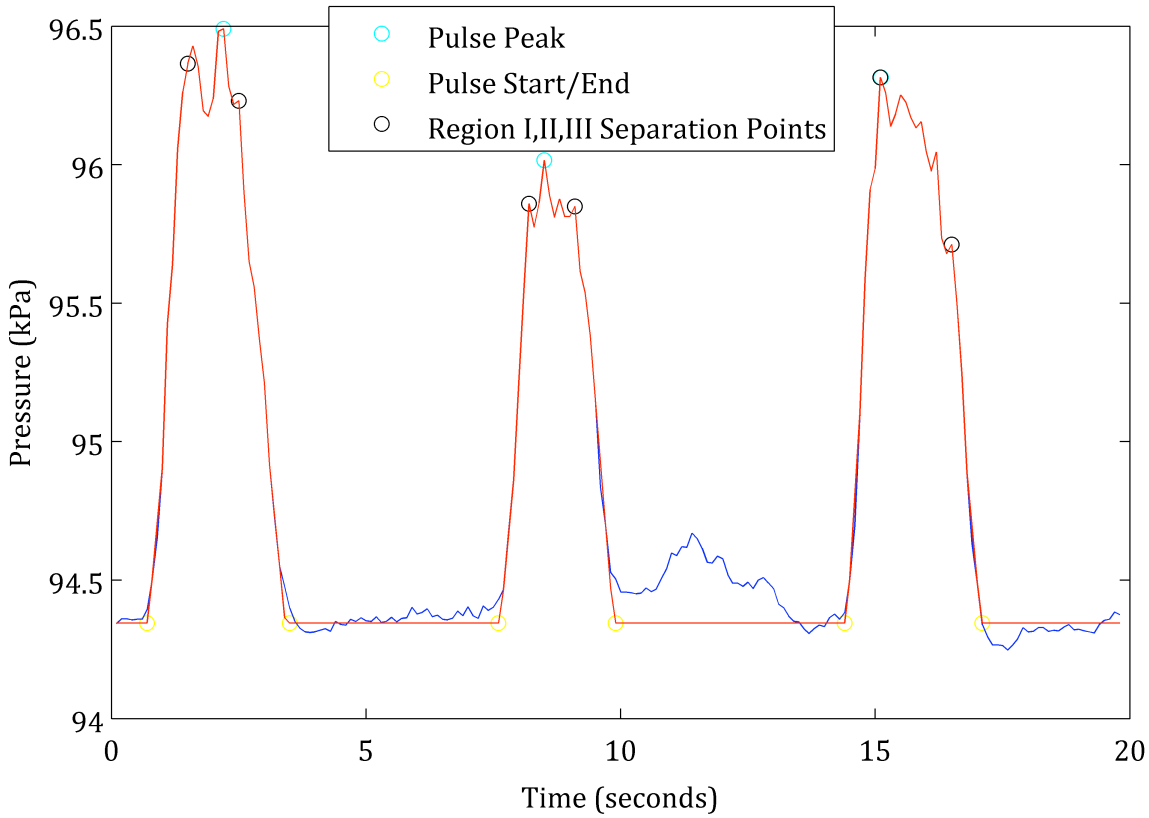

Figure 2.6: Results of filtering a raw data sample (blue) through the algorithm is shown (red). Primary pressure pulses are isolated from other pressure fluctuations. Peak pulse magnitudes, start and end locations of pulses, and points of transition between the three regions are identified.

In Figure 2.4b all data below the threshold value is discarded from analysis and the pulse is then extrapolated down to an averaged baseline pressure. This was necessary to select distinct beginning and ending points of pressure pulses that were not discernable, but these distinct points are simply approximations. In pressure traces where pulses exhibit magnitudes well above the threshold level these approximations are very close (Figure **2**.7). However, even in these cases the extrapolation technique does not account for the period in which the pressure drop at the end of some pulses gradually blends into the baseline pressure (Figure **2**.7). In data series where pulse magnitudes are very close to threshold values, the uncertainty associated with the approximations increases (Figure **2**.**8**), but the filtered pulse shapes still conform to visually observed trends.

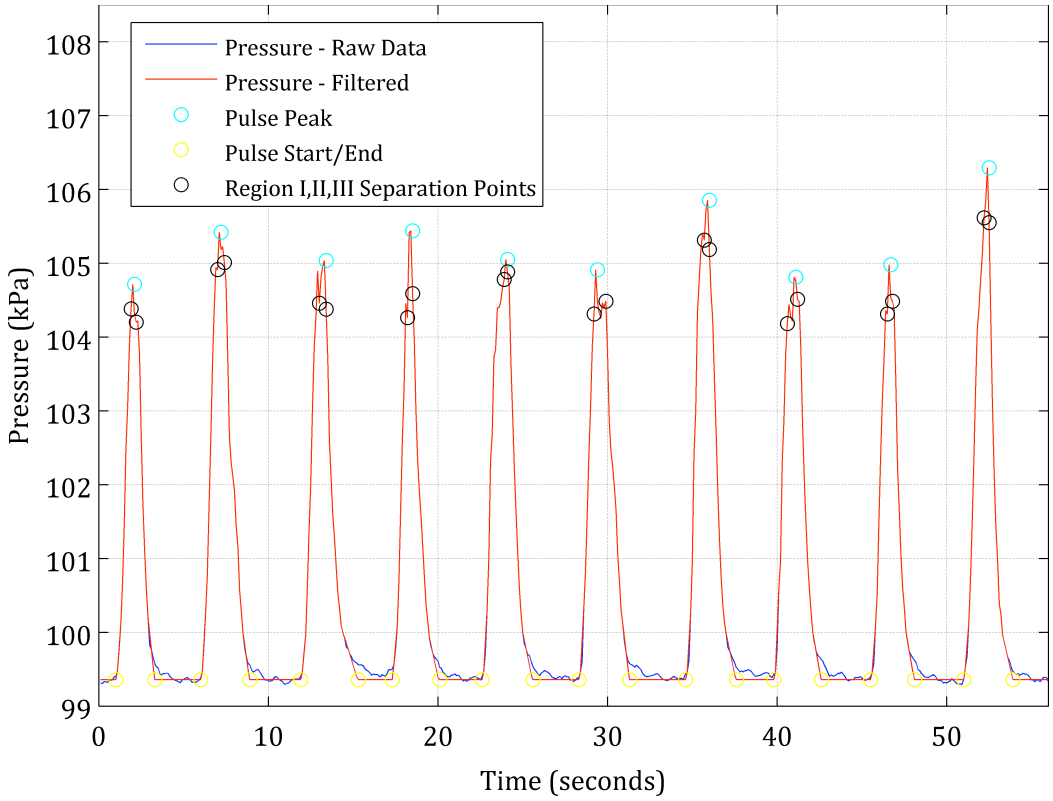

Figure 2.7: Example of filtering data with large pulse magnitudes. During instances of larger pulses magnitudes and minimal secondary fluctuations, the filter produces very close approximations of start, end, and region separation points. The terminal end of individual pulses where the pressure drops at a slower rate is excluded in the filtered data.

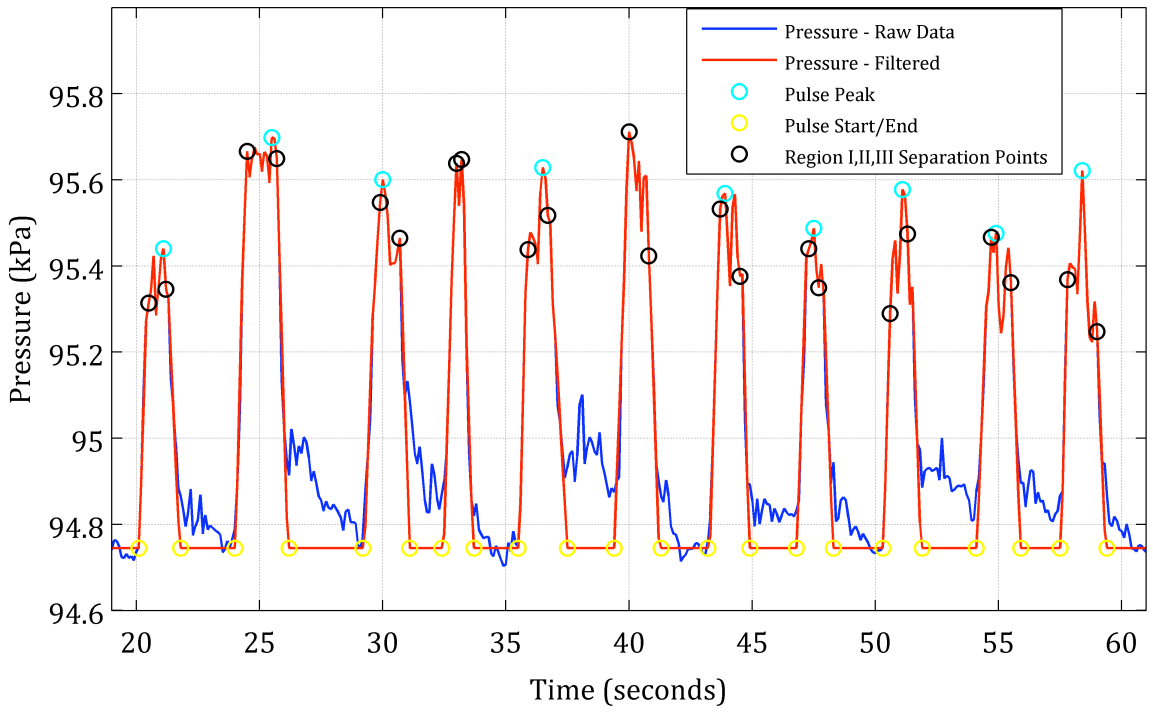

Figure 2.8: Example of filtering data with small pulse magnitudes. During instances of smaller pulse magnitudes, uncertainty increases in the filter's approximations of region separation points.

2.4.3 Comparing Instances of Tube Collapse to Pressure Patterns

In the x-ray trials, the videos synchronized with hemolymph pressure recordings taken during phase contrast imaging were reviewed, and each instance of filmed tube collapse was identified that did not coincide with bodily movements. To accomplish this, every occurrence of a tracheal tube collapse observed in the x-ray videos that was not accompanied by bodily motion was indicated by a pulse from a momentary on/off push button switch. The traces from the push button traces were then superimposed onto the pressure recordings. Using this method of pulse identification, the resulting trace obtain from the switch measurements was neither indicative of the collapse duration nor the precise timing of the collapse relative to the pressure pulse, but allowed us to investigate whether or not a pulse in hemolymph pressure accompanied each tube collapse.

Chapter 3 - Results

3.1 Box Trials

Two hours of the pressure recordings from each trial are displayed in Figure 3.1. All pressure and movement data for the box trials can be found in Appendix A.

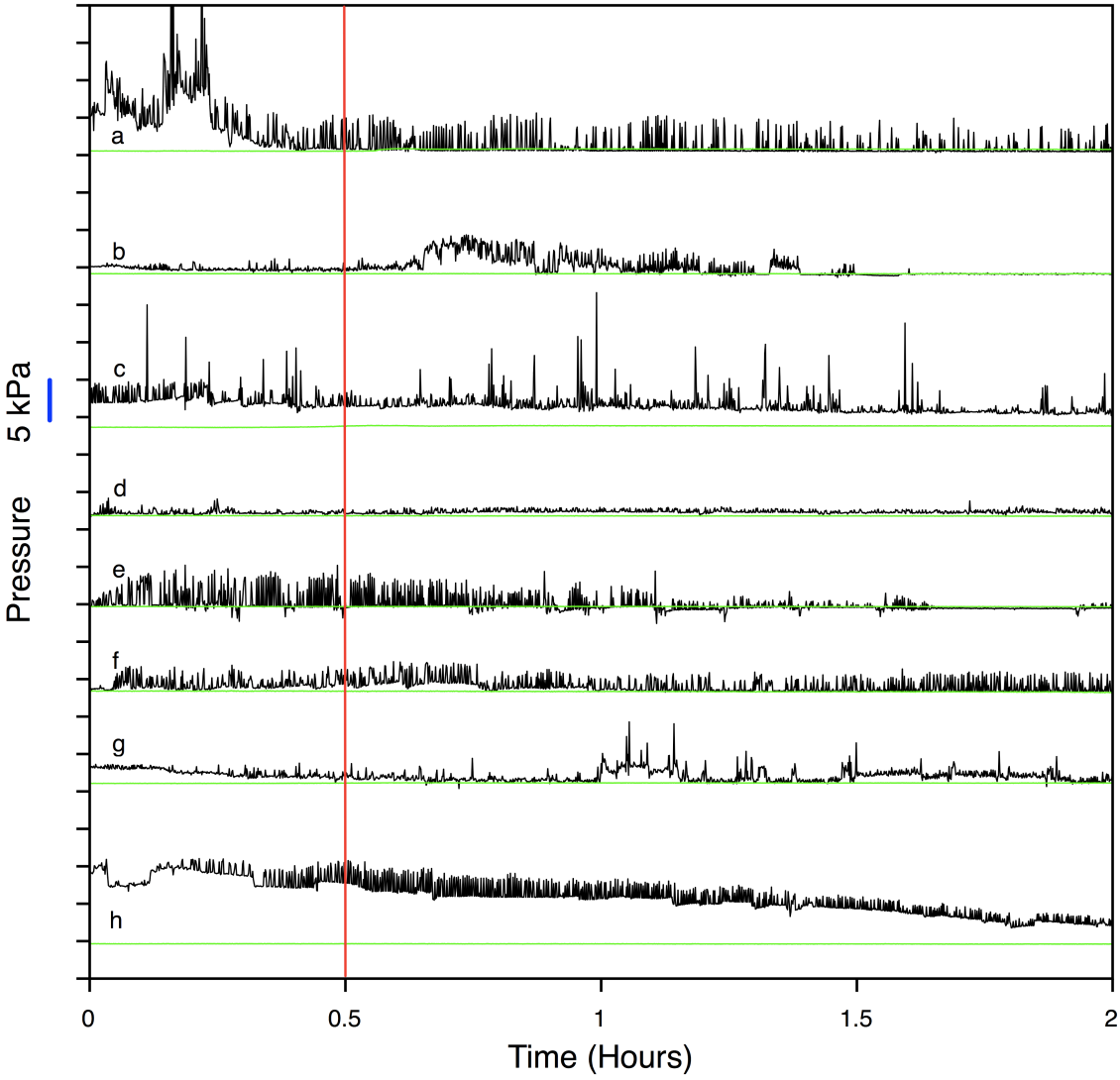

Figure 3.1: Two hour pressure recordings from the box trials. Hemolymph (black) and ambient (green) pressures from all trials are compared. The red line indicates the 30 minute recovery mark; only data after this point were analyzed.

Rhythmic pressure pulses are clearly observed to occur in the hemolymph of the prothorax of the beetles. During the initial recovery, pressure may fluctuate erratically (i.e. trace a), exhibit pressure pulses which increase steadily (i.e. trace e), maintain a short period of relative dormancy before exhibiting pulses (i.e. trace b, f, h), or display no obvious signs of recovery (i.e. trace c). The red line indicates the point at which animals have received 30 minutes of recovery since anesthetization. The behavior of the baseline pressure is variable between trials; it can remain fairly constant over large periods time (i.e. traces a, e, and f), undergo frequent shifts in magnitude (i.e. trace h), or exhibit behavior somewhere in between (i.e. traces b, c, d, and g). In four trials the baseline pressure remained consistently above ambient levels (i.e. trace c, d, g, h); in two trials the baseline maintained sub-ambient values (i.e. a, e); in the remaining two trials the baseline pressure exhibited values which fluctuate above and below atmospheric levels. The rhythmic nature of the pulses was disrupted during periods of large animal movements (Figure 3.2).

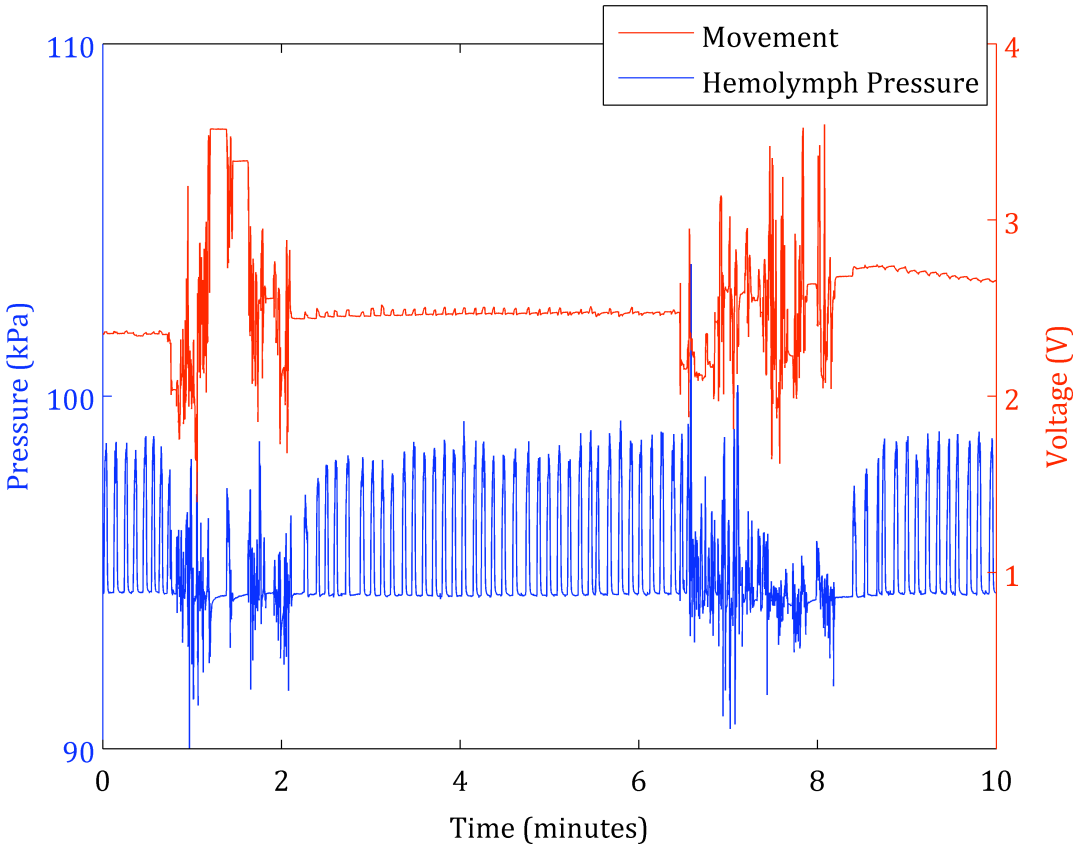

Figure 3.2: Effects of bodily movements. Rhythmic pulses in hemolymph pressure are disrupted during periods of large motion. Large-scale motion has been defined as any 0.2 Volt change in the recording of the optical sensor occurring over a 0.3 second window. This definition consistently identifies the observed patterns of movement.

The baseline pressure from which pulses tend to originate and terminate is seen to exhibit a fairly constant level in Figure 3.2. In the absence of large-scale movements, the optical sensor often indicated smaller scale movements that were not visible to the eye during experimentation (Figure 3.3).

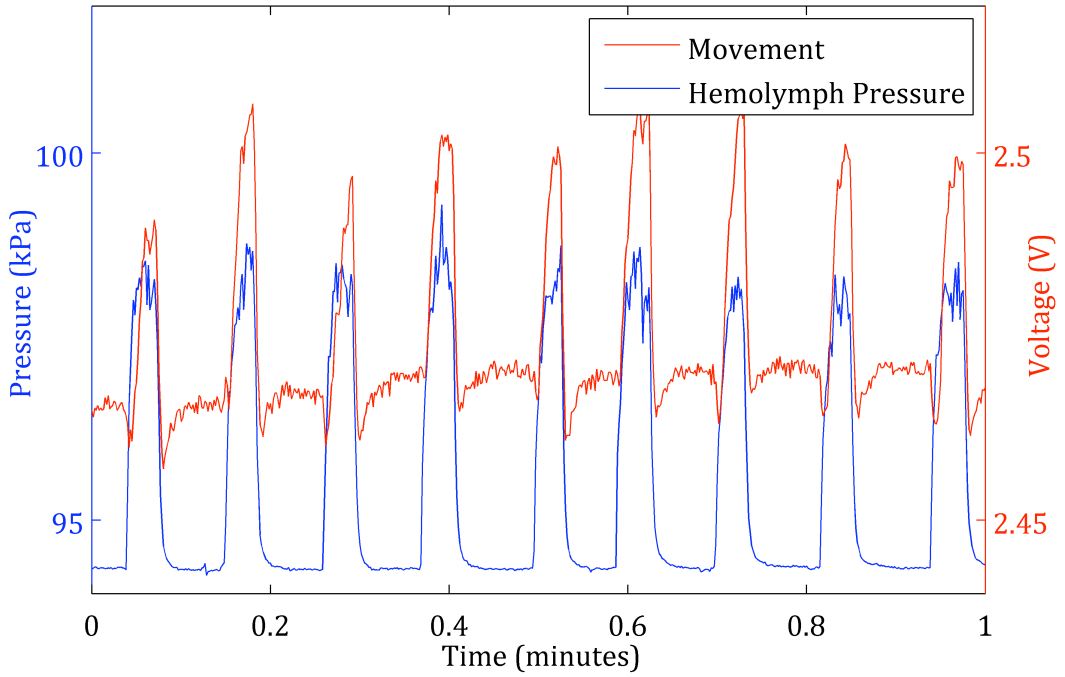

Figure 3.3: Small-scale movements are frequently observed. Rescaling the axes from the central portion of Figure 3.2 shows that small-scale movements co-occur with hemolymph pressure pulses.

These small movements are detected in all trials and are concurrent with pressure pulses. However, the small motions are not detected throughout the entirety of each trial. This may be due to the animal achieving an orientation that blocked the optical sensor from being able to detect certain movements.

Shifts in baseline pressure are present in all trials, to varying degrees. Changes in the baseline pressure were observed to occur in two manners: Sharp jumps accompanied by large-scale movement of the beetle, and gradual shifts over times that are not accompanied by movement. Figure **3.4** illustrates instances of abrupt changes in baseline hemolymph pressure concurrent with movement.

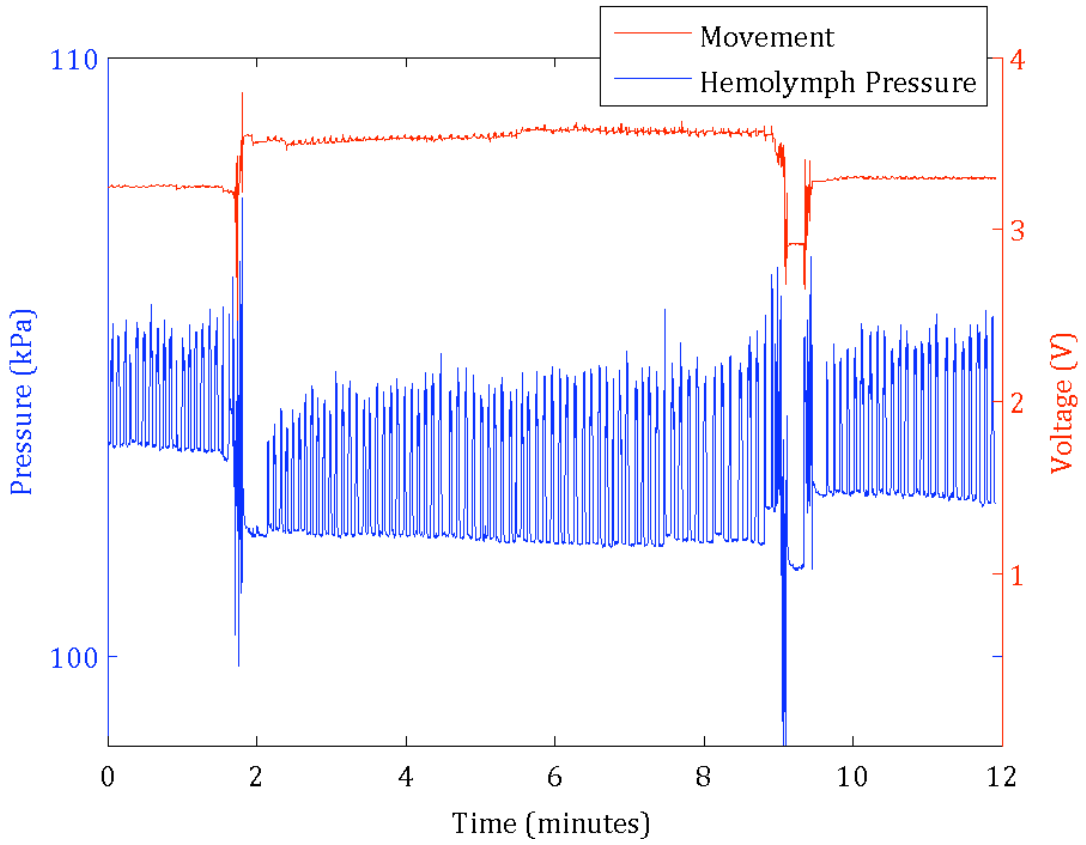

Figure 3.4: Abrupt changes in baseline hemolymph pressure correlated with large-scale movements. When movement occurs the pressure fluctuates erratically and exhibits a shift in the baseline pressure which, at the cessation of movement, can be either positive or negative.

In Figure **3**.**4**, instances of large movements are concurrent with interrupted rhythmic pulsations. At the conclusion of these particular movements the baseline pressure has shifted. Alternatively, Figure 3.5 shows an instance in which the baseline pressure is seen to gradually shift in the absence of movement (including small-scale movements).

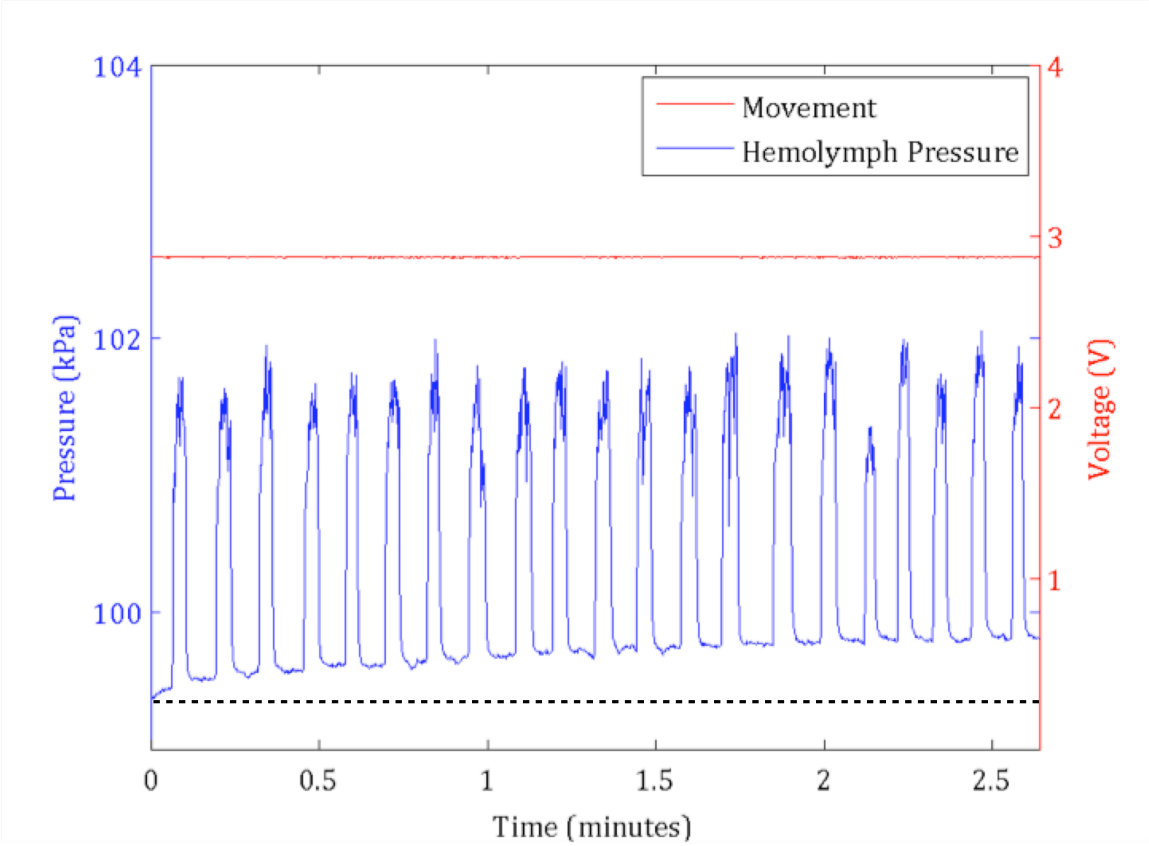

Figure 3.5: The baseline hemolymph pressure is observed to gradually shift over time, despite the absence of movement.

The calculated pressure pulse magnitudes as well as the frequency at which pressure pulses and tube collapses occur are compared in Figure 3.6, while the durations of the three different regions identified in the patterns of both pulses and tube collapses are compared in Figure 3.7. Pressure pulses are found to occur above atmospheric values. The frequency at which pulses and collapses occur, as well as the durations of the three respective regions are demonstrated to be very similar. Given the different species and experimental conditions from which these values are derived, the differences in magnitude are not significant.

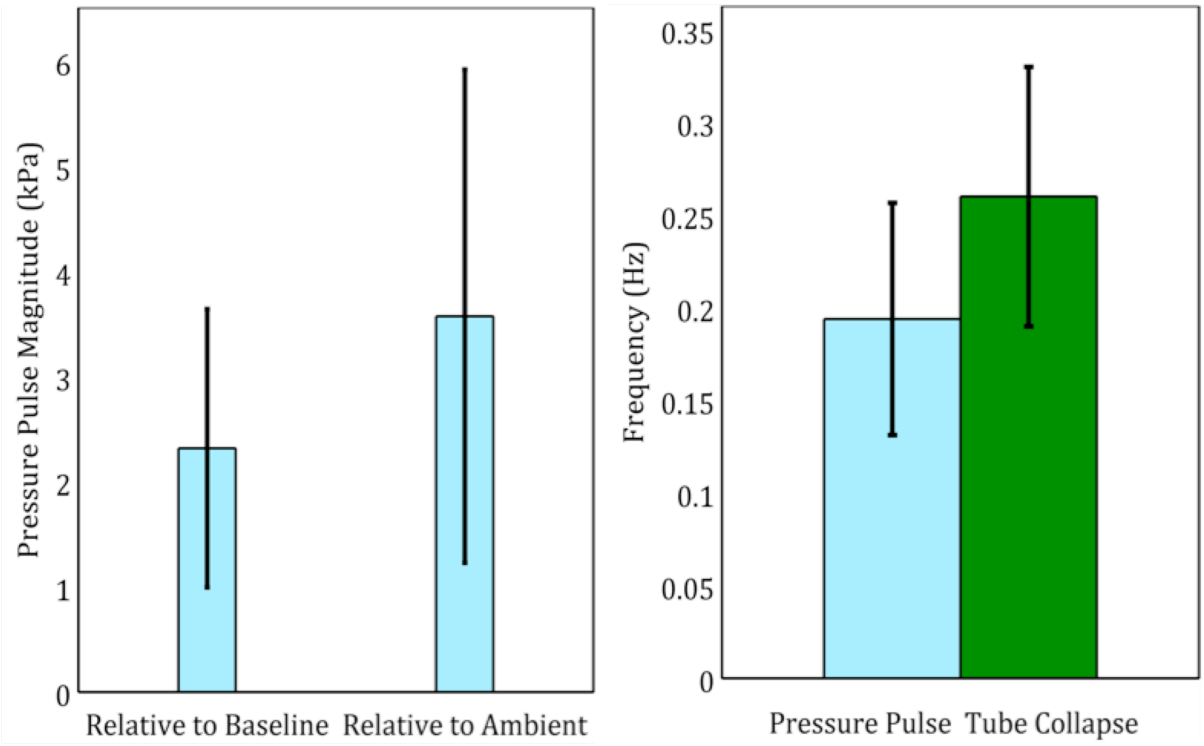

Figure 3.6: Comparison of both pulse magnitudes and the frequency at which pressure pulses and tube collapses occur. 400 pressure pulses (50 from each trial) were characterized. Colored boxes indicate the averaged values while the black lines indicate one standard deviation (same format is used hereafter). Tube collapse data published from Socha et al. [6]

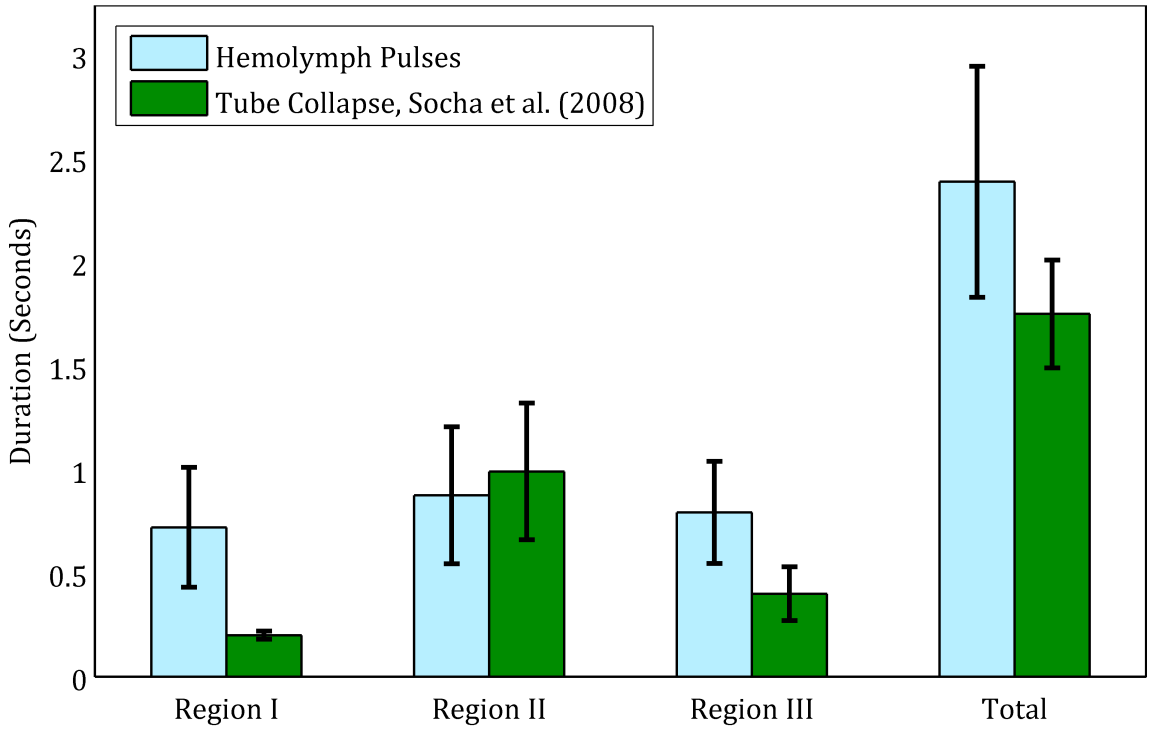

Figure 3.7: Durations of the three regions identified in the patterns of pressure pulses and tracheal tube collapses (Socha et al., 2008). 400 pressure pulses (50 from each trial) were characterized. Region I correlates to the period of pressure rise and decreasing tube width; Region II correlates to the period of fluctuating pressure with little net change and static tube collapse; Region III correlates to the period of dropping pressure and increasing tube width. Tube collapse data are from Socha et al. [6]

3.2 X-ray Trials

The hemolymph and ambient pressure traces recorded after the synchrotron beam was turned in each trial are shown in Figure 3.8. The complete traces can be found in Appendix B.

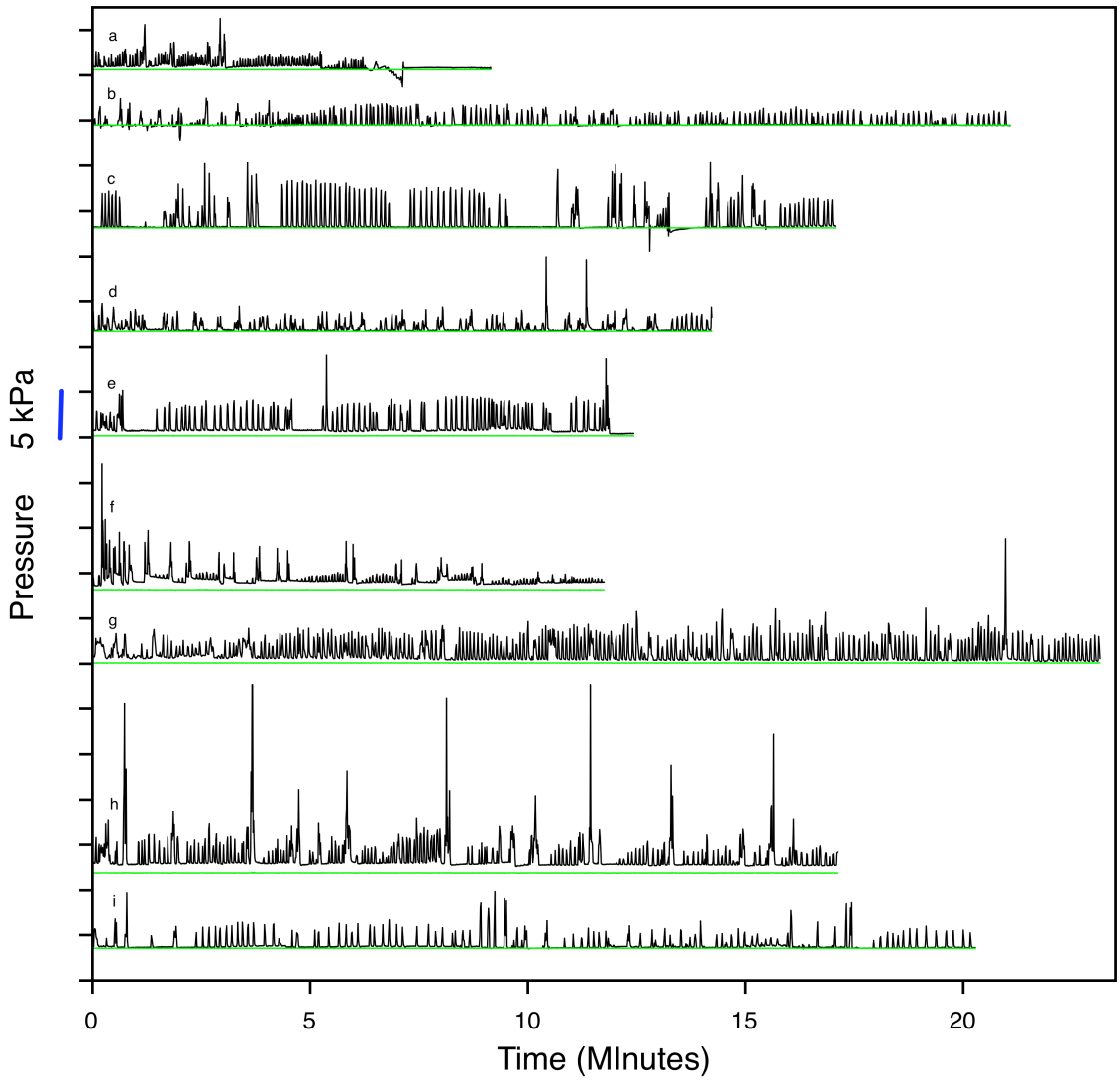

Figure 3.8: Pressure recordings taken during phase contrast imaging. Hemolymph (black) and ambient (green) pressures recorded after the synchrotron beam is turned on.

Pressure pulses similar to those observed during box trials are again present in the hemolymph pressure traces recorded during the x-ray trials. In this set of trials, the baseline pressure is more consistent. While it still exhibits both sharp and gradual shifts, it appears to do so more infrequently than observed in the box trials.

Videos taken of the insect tracheal system show rhythmic collapse and re-inflation of the tracheal system in each trial. Patterns of pressure and tube collapse are compared in Figure 3.9.

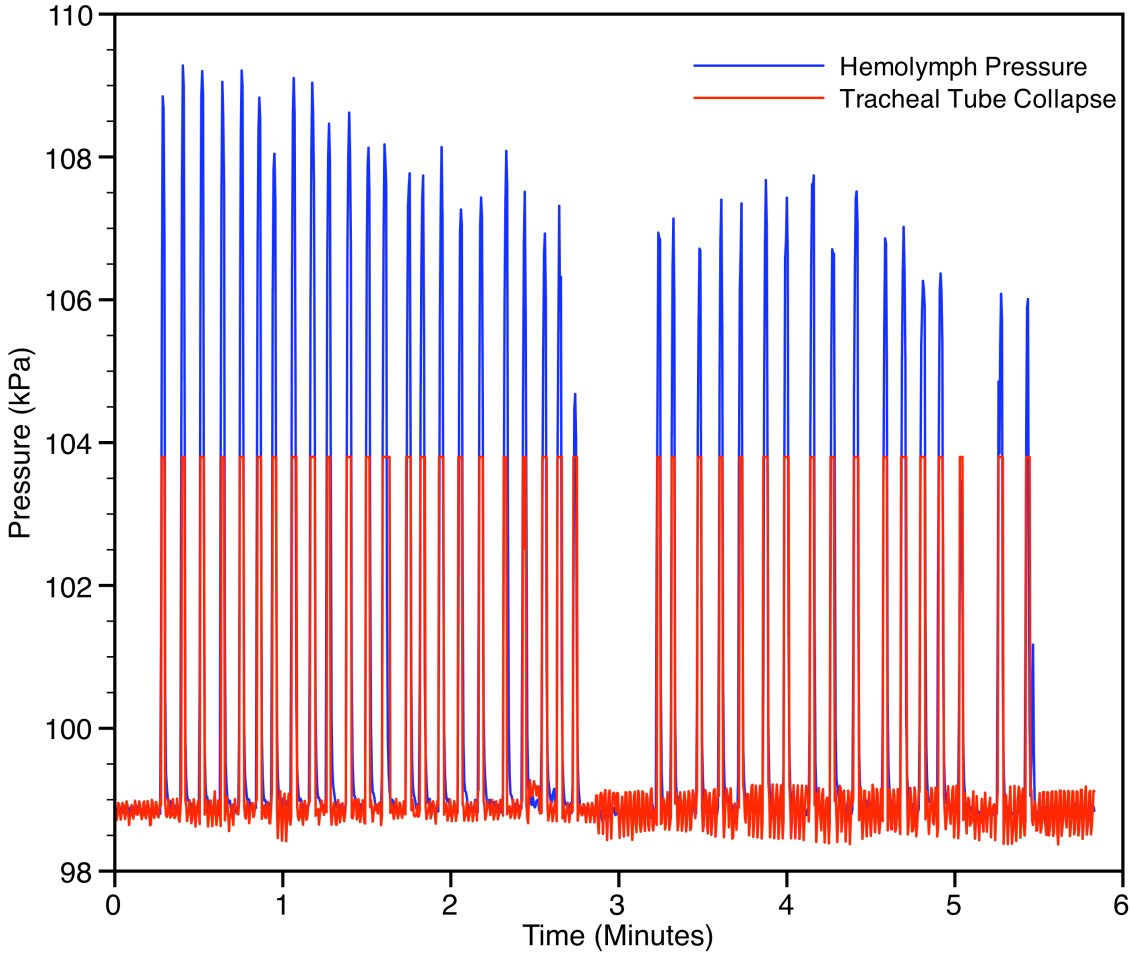

Figure 3.9: Relationship between pressure patterns and tube collapse. Using synchronized video and pressure recordings, pressure pulses are observed to accompany tracheal tube collapse.

Hemolymph pressure pulsations and tracheal tube collapse are consistently observed to co-occur. Videos from all trials in Figure 3.8 have been analyzed, and at no point is a tracheal tube collapse observed that is not accompanied by a pressure pulse.

3.3 Data Comparison

Ten pulses from each of the x-ray trials (90 total) were characterized and contrasted with the results of characterizing pulses from the box trials. A comparison demonstrates that the patterns of pulse durations are very similar in the two trials (Figure **3.10**), but the pulse magnitudes exhibit differences (Figure 3.11).

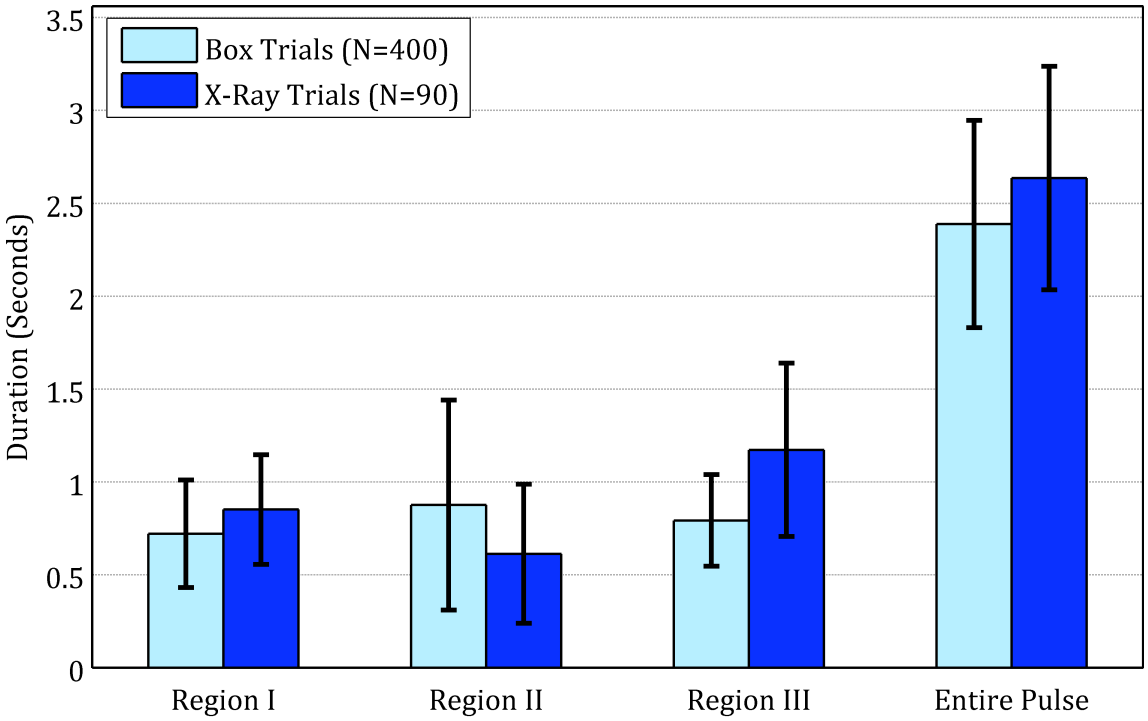

Figure 3.10: Patterns in pulse durations are similar in the two experiments.

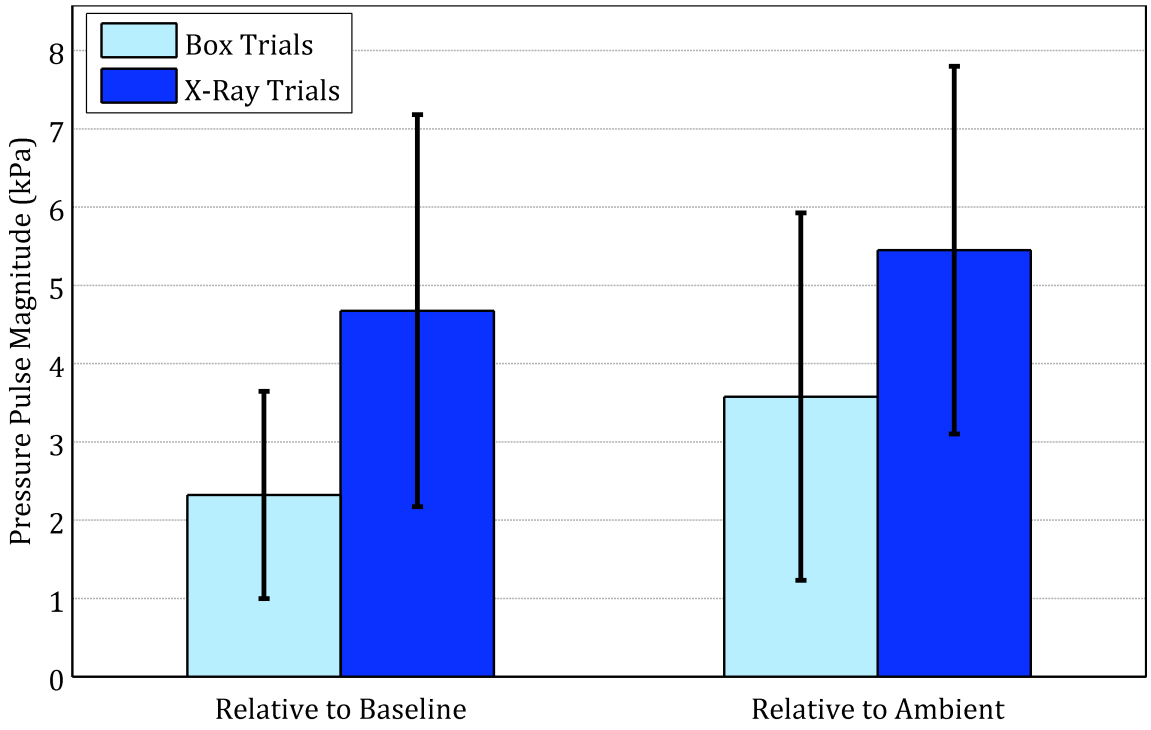

Figure 3.11: Differences in the pressure magnitudes are observed in the box and x-ray trials. Pulse magnitudes relative to both the baseline and ambient pressures tend to be larger in the x-ray trials.

To provide insight into the importance of pulse magnitudes, a data sub-set containing the smallest pressure pulses recorded during footage of the primary tracheal tubes was selected and compared with tracheal tube collapse (Figure 3.12).

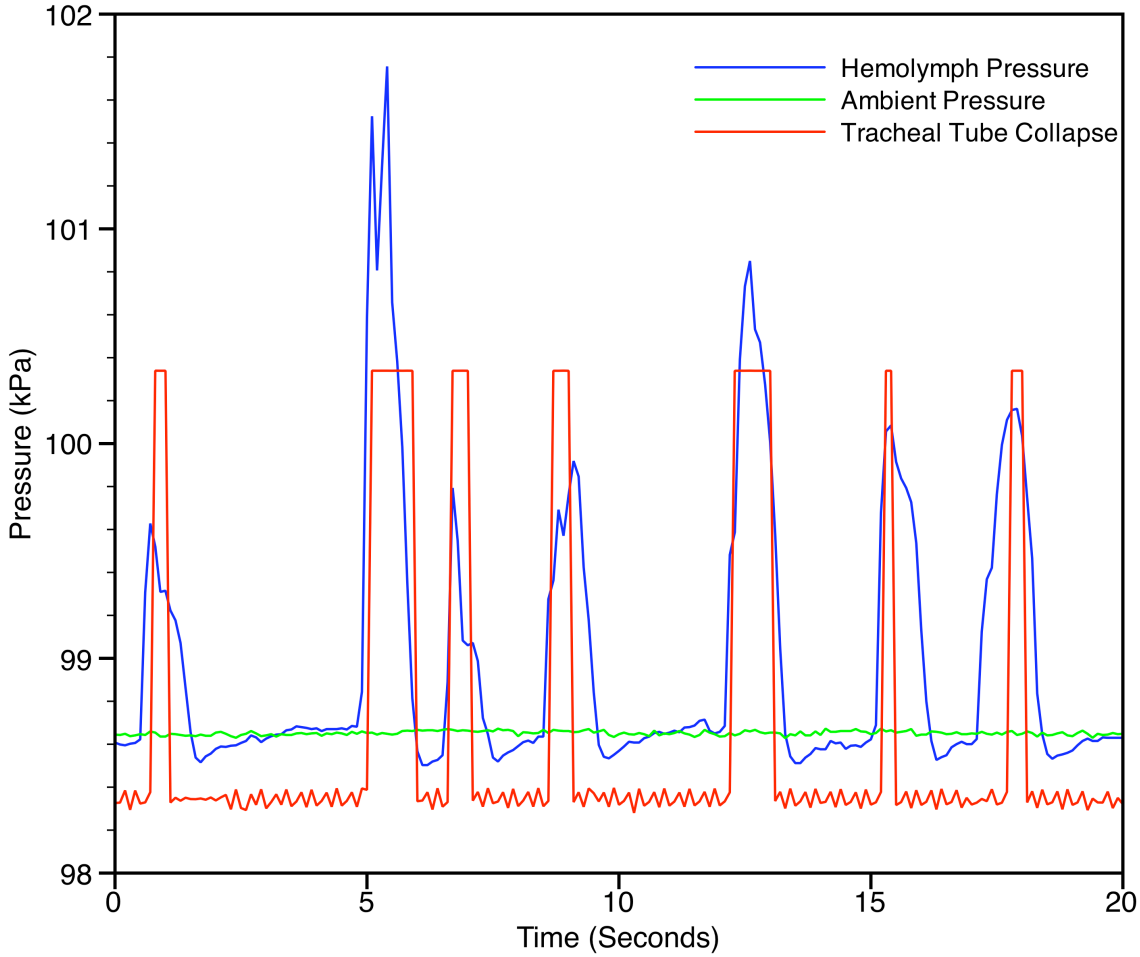

Figure 3.12: A data segment from the x-ray trials in which hemolymph pressure pulses exhibit both relative and absolute peak magnitudes over one standard deviation smaller than the average magnitudes recorded during the box trials. A pulse in the red line indicates that the primary tracheal tubes have collapsed. While this red trace does not accurately represent of the collapse duration or timing, it demonstrates that collapse does occur in the presence of the smaller pressure pulses on the order of 1 kPa.

While the hemolymph pressure pulses tended to be larger during the x-ray trials, Figure 3.12 demonstrates that the primary tracheal tubes collapsed in the presence of small pressure pulses exhibiting peak magnitudes relative to both baseline and ambient pressure on the order of 1 kPa. The full set of pulse parameters characterized in each experiment is detailed in Table **1**.

Table 1: Summary of pressure pulsations. Values shown are the mean +/- the standard deviation.

	Box Trials	X-Ray Trials
Magnitude Relative to Baseline	2.32 +/- 1.32 kPa	4.67 +/- 2.51 kPa
Magnitude Relative to Ambient	3.58 +/- 2.35 kPa	5.45 +/- 2.35 kPa
Total Duration	2.4 +/- 0.6 s	2.6 +/- 0.6 s
Region I: Duration	0.7 +/- 0.3 s	0.85 +/- 0.3 s
Region II: Duration	0.9 +/- 0.6 s	0.6 +/- 0.4 s
Region III: Duration	0.8 +/- 0.2 s	1.2 +/- 0.5 s
Region I: Rate of Increase	2.8 +/- 1.6 kPa/s	4.9 +/- 2.5 kPa/s
Region III: Rate of Decrease	2.7 +/- 1.6 kPa/s	3.6 +/- 1.7 kPa/s
Frequency	11.6 +/- 3.8 pulses/min	10.6 +/- 4.0 pulses/min

Chapter 4 - Discussion

4.1 Comparison of Changes in Pressure and Tube Morphology

We hypothesized that pressure pulses reaching magnitudes above that of the ambient pressure existed in the beetles' hemolymph, the patterns of which would be similar to those of previously observed tube collapse. Pressure recordings taken during the box trials measured above atmospheric pulses and showed that the frequency of these pulses were similar to the frequency of tube collapse and reinflation [6]. A more thorough comparison was done relating the durations of patterns in pressure to patterns of morphological changes in tracheal tubes. Specifically, the region of pressure rise was compared to the region of decreasing tube diameter, the region of fluctuating pressure with little net change to the region of static tube collapse, and the region of decreasing pressure to that of increasing tube diameter. Comparing these regions is an imperfect method since it assumes the three regions would match up. In reality, a tube might not begin to collapse until a certain pressure threshold is reached and may fully collapse at a low pressure while the pressure pulse continues to rise, thus creating a time lag in the onset of different regions of pressure pulses and tube collapse. Despite this as well as differences in experimental conditions and the species used, all values are of the same order of magnitude and are relatively close in value.

4.2 Correlation of Pressure Pulses and Tube Collapse

We hypothesized that the mechanism driving collapse of tracheal tubes is a pressure difference imposed across tracheal tube walls by fluctuating hemolymph pressures. Accordingly, we expected that a pulse in hemolymph pressure would accompany every instance of tube collapse. Observations of the x-ray videos show that some, but not all, portions of the tracheal system rhythmically collapse throughout the

insects' body concurrently collapse. Comparing the instances of tracheal tube collapse to the simultaneously recorded pressure pulses demonstrates that the two consistently occur together. As hypothesized, no instance of tube collapse is observed that is not accompanied by a pressure pulse. A strong relationship between pressure pulses and hemolymph circulation has been previously demonstrated in tenebrionid beetles [14], suggesting that there may be a fundamental coupling in the functionality of hemolymph pressure pulsations, to augment transport of both air and hemolymph .

4.3 Effects of Experimental Conditions on Hemolymph Pressure

To the best of our knowledge, the characterization of pressure patterns in each experiment provides the first descriptive analyses of directly measured hemolymph pressure patterns in insects (Table 1). The analyses of hemolymph pressures are relevant to two experimental conditions. The setup used in the box trials attempted to impose as few constraints as possible on the beetles while performing direct measurements of hemolymph pressure. In the x-ray experiment however, insects are heavily (though not completely) surrounded by adhesive putty to immobilize them while they are subjected to synchrotron radiation and x-ray videos are captured. Thus, the characterization of pressure in the box trials likely gives superior insight into the hemolymph environment of beetles in their natural state.

The characterization of pressure patterns quantifies differences in the hemolymph environment due to the experimental conditions. Both the total duration and durations of individual pulse regions exhibit similar values in the two experiments. In the x-ray experiments, however, the average magnitudes of pressure pulses relative to both baseline and ambient pressures were larger than those observed in the box experiment. To account for this, a data subset was chosen from an x-ray trial that contained the smallest pressure pulses that were recorded during a period of time where the camera observed the primary tracheal tubes. This latter condition was important since the camera was not relegated to observing only the primary tracheal tubes in the thorax. Because it is unknown whether the hemolymph pressure changes uniformly throughout the entirety of the insects' body, footage of the primary tracheal tubes was chosen for comparison between experiments since they are located in the same vicinity as the pressure

transducer. The voltage trace plotted alongside the pressure in Figure 3.12 shows that compression of the primary tracheal tubes is accompanied by pressure pulses of smaller magnitudes than the averages recorded in the box trials. In fact, the first pulse shown in Figure 3.12 exhibits a magnitude of 1.01 kPa and is more than one standard deviation below the relative average magnitudes calculated in the box trials. This relationship suggests that tracheal tube collapse consistently occurred during the box trials and supports the hypothesis that rhythmic tracheal collapse is a phenomenon utilized by carabid beetles in their natural environment.

4.4 Assessment of Pulse Magnitudes and Baseline Pressure

Pulse magnitude relative to the ambient pressure and the pulse magnitude relative to the baseline hemolymph pressure are calculated throughout this study in lieu of reporting the ideal parameter: pulse magnitude relative to intra-tracheal pressure, which quantifies the pressure gradient across the walls of the tracheal tubes. Although intra-tracheal pressures were not directly measured in these experiments, previous studies have shown that intra-tracheal pressure tends to remain at atmospheric levels just inside the spiracles, while they are opened, and will periodically fluctuate around this value [7-10]. Due to the diffusion of gases throughout the tracheal system, we would not expect the atmospheric pressure values, taken immediately inside of a spiracle, to be indicative of the pressure throughout the tracheal system. However, if we assume that the pressure inside of the larger tracheal tubes, where we observe collapse to occur, is equivalent to the pressure just inside of the spiracle, then we expect that the pulse magnitude relative to the ambient pressure reflects the actual pressure gradient across the walls of tracheal tubes.

Because previous studies have reported consistent baseline pressures [10, 13], the observed shifts in baseline pressure have caused us to question the accuracy of our pressure recordings. In all trials, sudden shifts in baseline pressure occur after periods of motion. The reason for these shifts is not known. One possibility is that beetles employ some unknown physiological mechanism capable of quickly shifting the baseline hemolymph pressures. It is also possible that beetles can push themselves against physical constraints, compressing their bodies and increasing the baseline pressure. In

either of these cases, we would expect pulse magnitude relative to the ambient pressure to be a good approximation of pressure gradients across tube walls, so long as our assumption of an atmospheric pressure inside the large tubes is valid.

Alternatively, physical impingement of the pressure transducer could account for the changes. The anatomy of carabid beetles is such that a number of tissues or tracheal tubes may be able to press against the membrane of the transducer. A local stress applied to the transducer membrane could result in incorrect measurements of absolute pressure and a shifted baseline pressure. The degree of impingement could be expected to change if the beetle moves, and shifts in baseline pressure are observed to occur concurrently with movement. In the box trials, which allowed for significantly more body movement than in the x-ray trials, we observed larger shifts in baseline pressure (Figure 3.1h). This is consistent with the hypothesis that baseline shifts occur due to movement of the beetle (or its internal structures) relative to the transducer. If, in reality, the hemolymph pressure maintains a consistent baseline throughout the trials and observed shifts in the baseline are the result of inaccurate absolute pressure measurements caused by locally applied stresses, then the pressure magnitude relative to the baseline may better reflect the pressure gradients across tracheal tube walls, so long as our assumption of an atmospheric pressure inside the larger tubes is valid. To approximate the pressure gradients across tubes using the pressures relative to the baseline it would simply be necessary to quantify what the stable baseline pressure is in the carabid beetles. The difference between the ambient values and the (theoretical) stable baseline would simply need to be added to the values recorded by our transducers. Slama [13] inferred a consistent sub-atmospheric hemolymph pressure in larva using external strain gauges. Direct pressure measurements published by Ichikawa [14] appear to display a consistent baseline pressure slightly above atmospheric values. Unfortunately, if the true baseline pressure does remain consistent throughout trials in this study and exhibits a similar magnitude between individual carabid beetles, it is not easily identified in the data sets. In the x-ray trials where movement was less frequent, 8 of the 9 trials exhibited baseline pressures consistently above atmospheric levels. But of these trials, 3 maintained baseline pressures within 0.5 kPa above ambient values (one of which briefly exhibited a sub-ambient baseline) and 3 were consistently within 1 kPa. In two trials baseline pressures

consistently 2 kPa and 3 kPa above ambient values were recorded. In only one trial were subambient baseline pressures recorded to be approximately -0.05 kPa of atmospheric values. From this widely variable data we can at most infer that if a similar baseline pressure exists across carabid beetles it is likely above the ambient pressure.

4.5 Summary

In conclusion, the results of this study provide new insight into the relationship between pressure pulses and the collapse of tracheal tubes. The consistency with which pressure pulses accompany tube collapse supports the hypothesis that patterns in hemolymph pressure are the mechanism driving rhythmic tracheal collapse. The comparison of pressure patterns in the box and x-ray experiments suggests that pressure pulses are capable of driving tracheal collapse outside of the experimental conditions needed to observe it. Finally, the method of characterizing pulses developed in this study provides the first quantitative descriptions of the hemolymph pressure environment in carabid beetles.

References

1. Weis-Fogh, T., *Diffusion In Insect Wing Muscle, The Most Active Tissue Known.* Journal of Experimental Biology, 1964. 41(2 %U http://jeb.biologists.org/content/41/2/229.abstract): p. 229-256.
2. Krogh, A., *Studien über Tracheenrespiration.* Pflügers Archiv European Journal of Physiology, 1920. 179(1): p. 95-112.
3. Miller, P.L., *The Regulation of Breathing in Insects.* Advances in Insect Physiology, 1966. Volume 3: p. 279-354.
4. Buck, J., *Some physical aspects of insect respiration.* Annu. Rev. Entomol, 1962. 7: p. 27-56.
5. Westneat, M.W., et al., *Tracheal Respiration in Insects Visualized with Synchrotron X-ray Imaging.* Science, 2003. 299(5606 %U http://www.sciencemag.org/content/299/5606/558.abstract): p. 558-560.
6. Socha, J.J., et al., *Correlated patterns of tracheal compression and convective gas exchange in a carabid beetle.* Journal of Experimental Biology, 2008. 211(21): p. 3409-3420.
7. Levy, R.I. and H.A. Schneiderman, *Discontinuous respiration in insects--IV. Changes in intratracheal pressure during the respiratory cycle of silkworm pupae.* Journal of Insect Physiology, 1966. 12(4): p. 465-492.
8. Lighton, J.R.B., *Discontinuous Ventilation in Terrestrial Insects.* Physiological Zoology, 1994. 67(1): p. 21.
9. Miller, P.L., *Respiration: aerial gas transport. In The Physiology of Insects. .* New York: Academic Press. , 1974. 4: p. 345-402.
10. Duncan, F.D., T.D. Fˆrster, and S.K. Hetz, *Pump out the volume--The effect of tracheal and subelytral pressure pulses on convective gas exchange in a dung beetle, Circellium bacchus (Fabricus).* Journal of Insect Physiology, 2010. 56(5): p. 551-558.
11. HARRISON, J.F., *Ventilatory Mechanism and Control in Grasshoppers.* American Zoologist, 1997. 37(1): p. 73-81.
12. Miller, P.L., *Rhythmic activity in the insect nervous system: Thoracic ventilation in non-flying beetles.* Journal of Insect Physiology, 1971. 17(3): p. 395-405.
13. Sláma, K., *Recording of haemolymph pressure pulsations from the insect body surface.* Journal of Comparative Physiology B: Biochemical, Systemic, and Environmental Physiology, 1984. 154(6): p. 635-643.
14. Ichikawa, T., *Periodic abdominal pumping supports leg development during metamorphosis in tenebrionid beetle Zophobas atratus.* Comparative Biochemistry and Physiology - Part A: Molecular & Integrative Physiology, 2008. 150(1): p. 8-13.
15. Socha, J., et al., *Real-time phase-contrast x-ray imaging: a new technique for the study of animal form and function.* BMC Biology, 2007. 5(1): p. 6.

Appendix A – Complete Data Sets From Box Trials

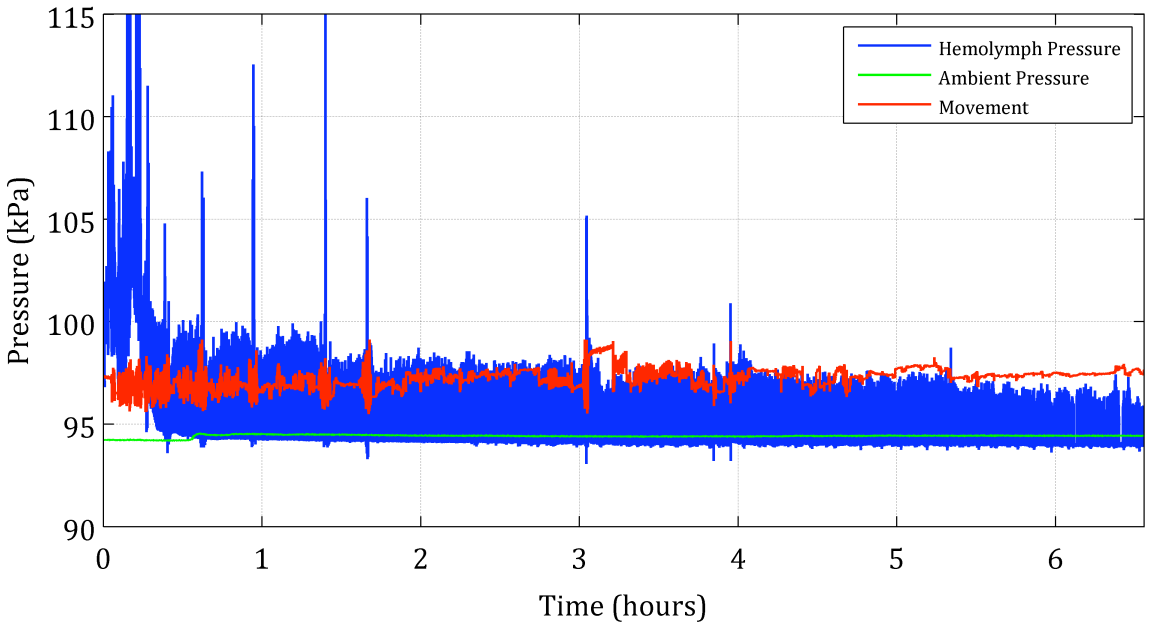

Figure A.1: Raw data associated with the pressure trace in Figure 3.1a

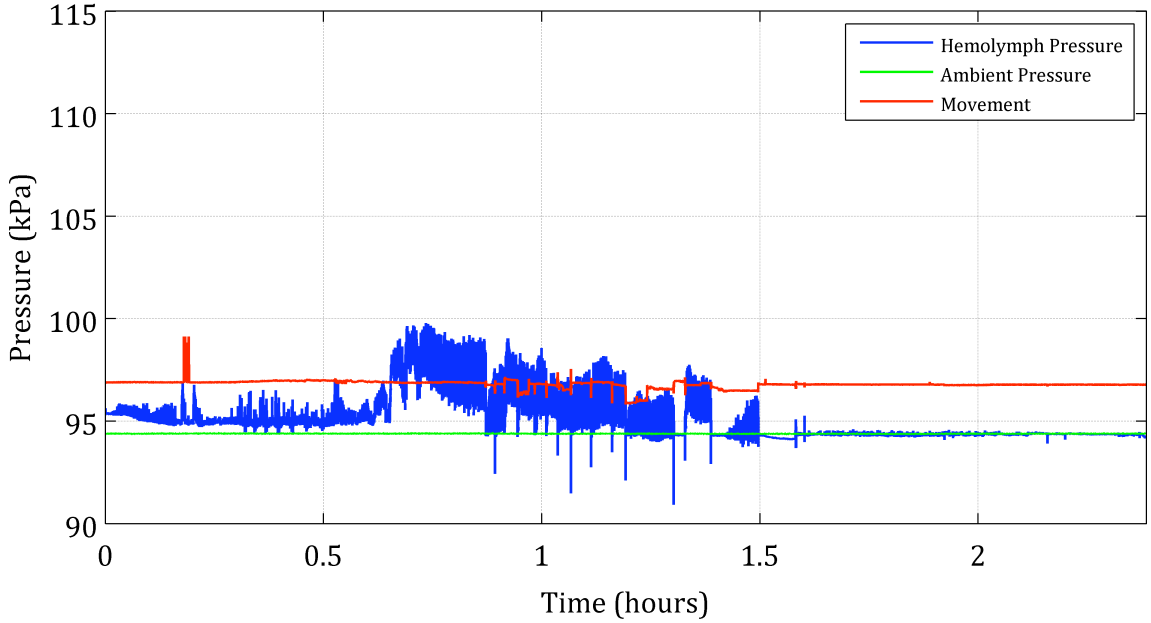

Figure A.2: Raw data associated with pressure trace in Figure 3.1b

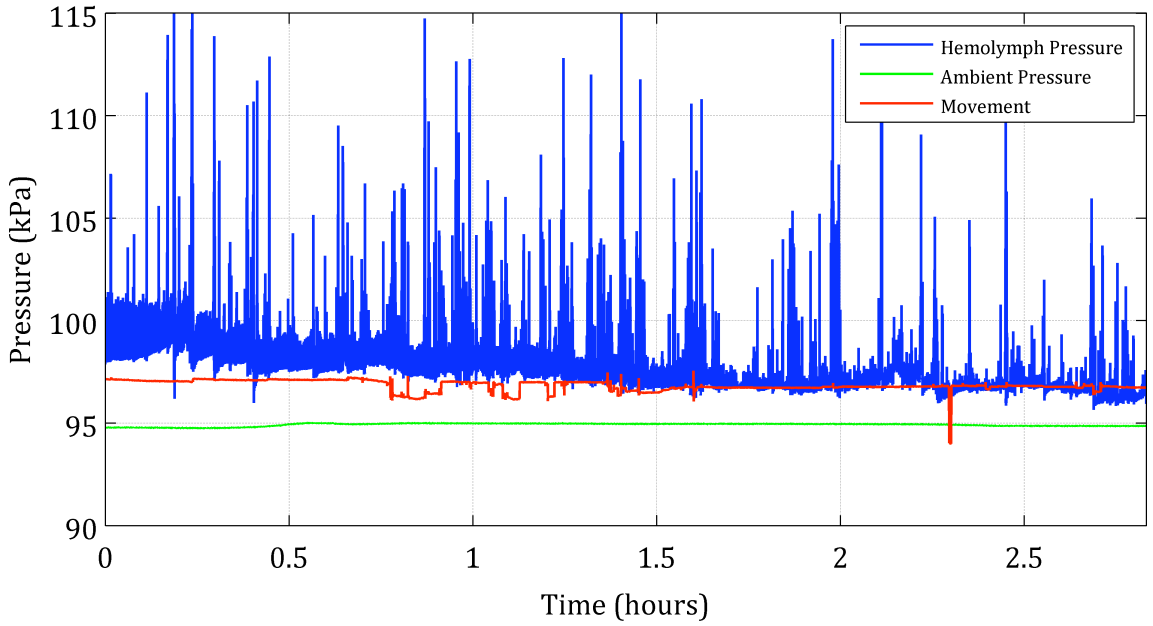

Figure A.3: Raw data associated with pressure trace in Figure 3.1c

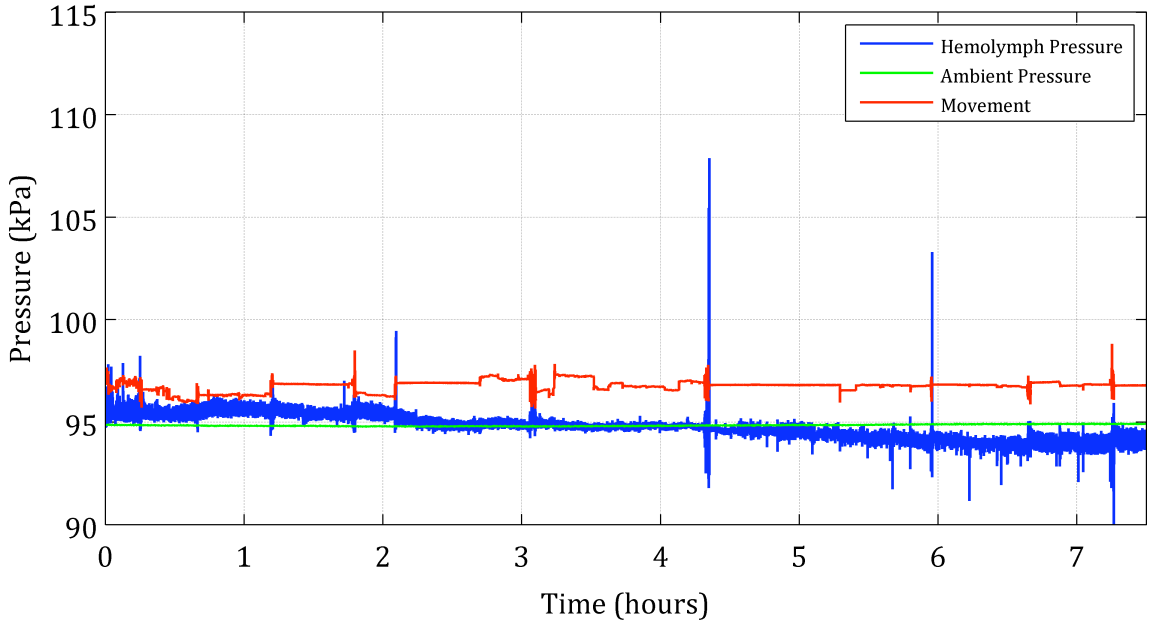

Figure A.4: Raw data associated with pressure trace in Figure 3.1d

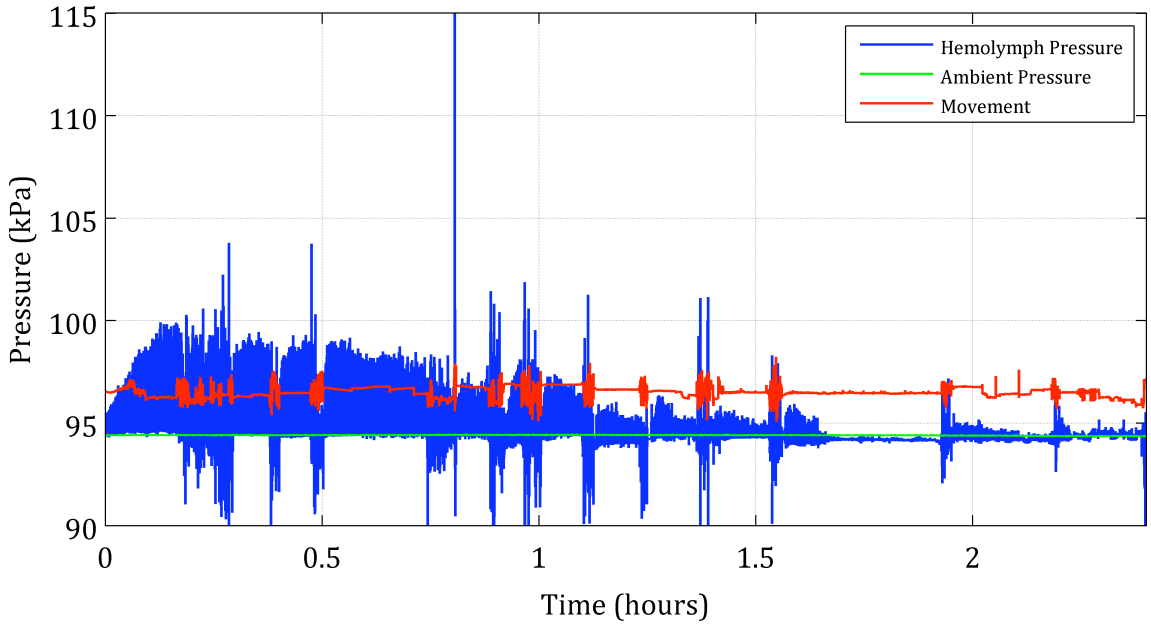

Figure A.5: Raw data associated with pressure trace in Figure 3.1e

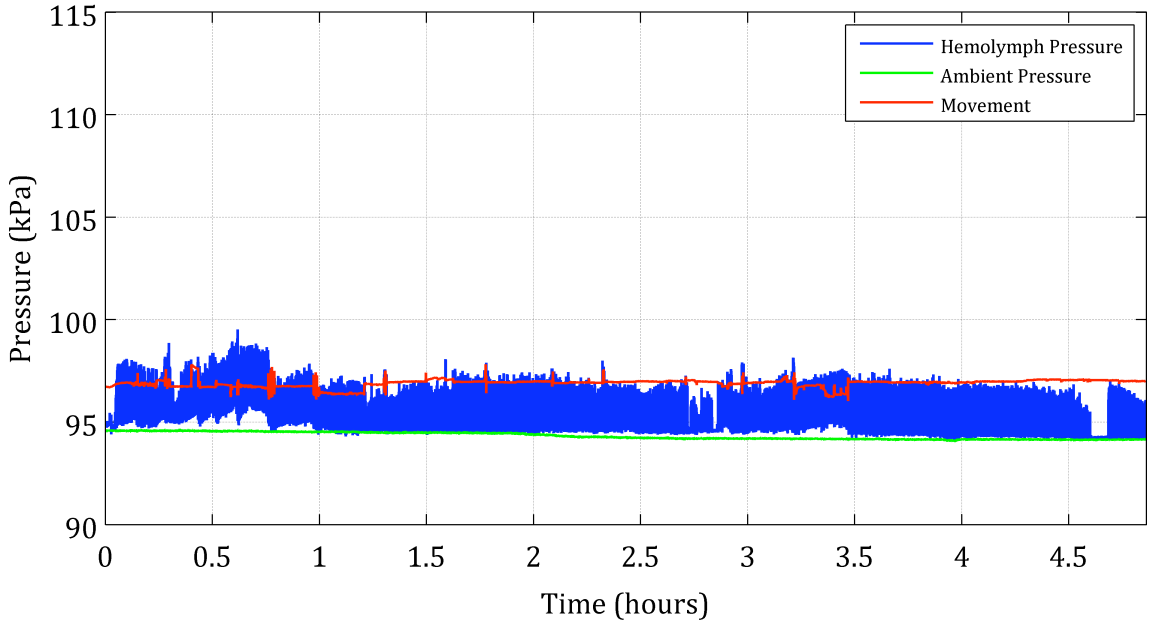

Figure A.6: Raw data associated with pressure trace in Figure 3.1f

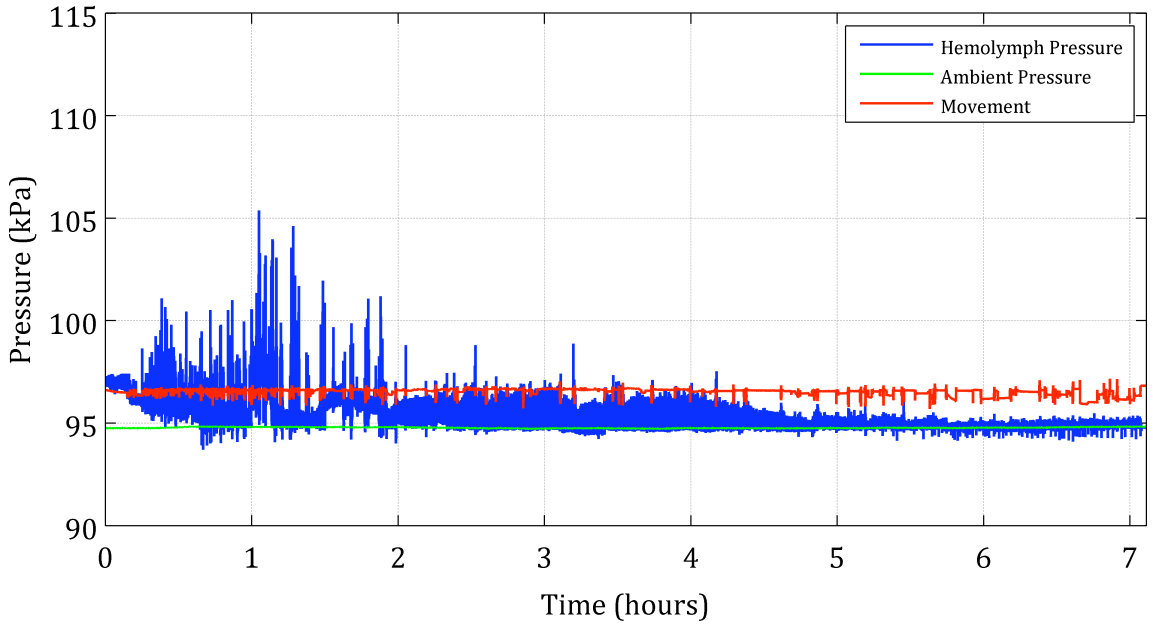

Figure A.7: Raw data associated with pressure trace in Figure 3.1g

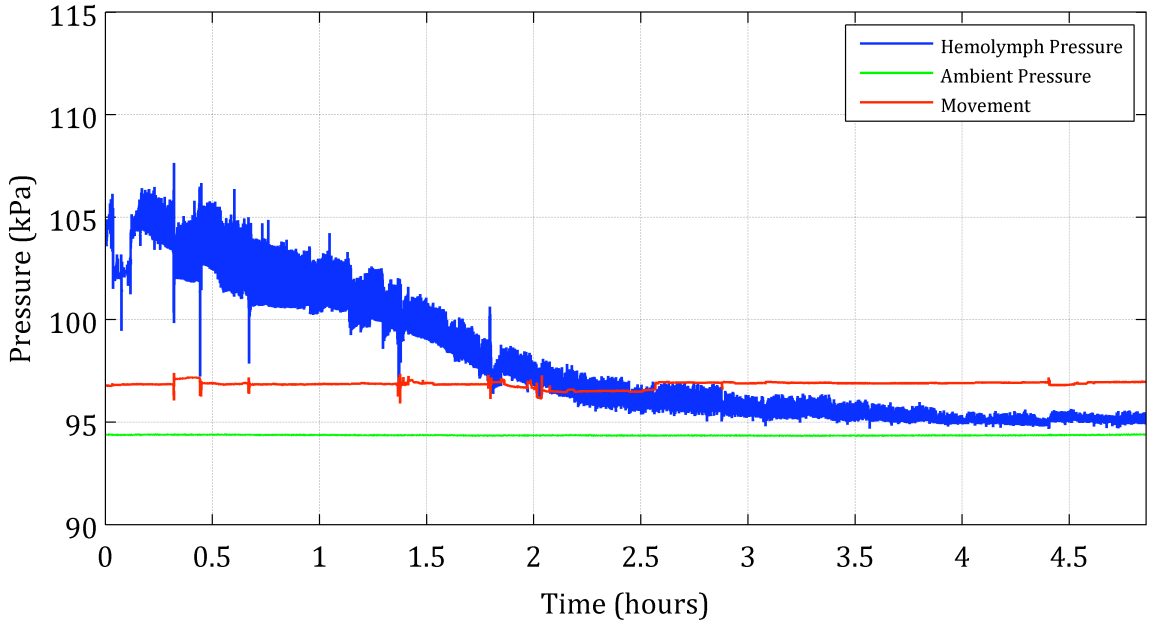

Figure A.8: Raw data associated with pressure trace in Figure 3.1h

Appendix B - Complete Data Sets From X-ray Trials

Some of the data contained in this appendix was not characterized. The initial portions of each plot contain periods where both of the sensors used in the experiment record ambient pressures. Following this, rapid pressure fluctuations may be seen in the hemolymph recording as the pressure sensor is physically inserted into the beetles thorax and then sealed. Neither of these periods is indicated in the plots. After this point each plot contains a data segment where hemolymph is recorded in the absence of synchrotron radiation. The black bar in each graph indicates the point at which the synchrotron beamline is turned on and imaging began. Only data after this black line was considered for characterization.

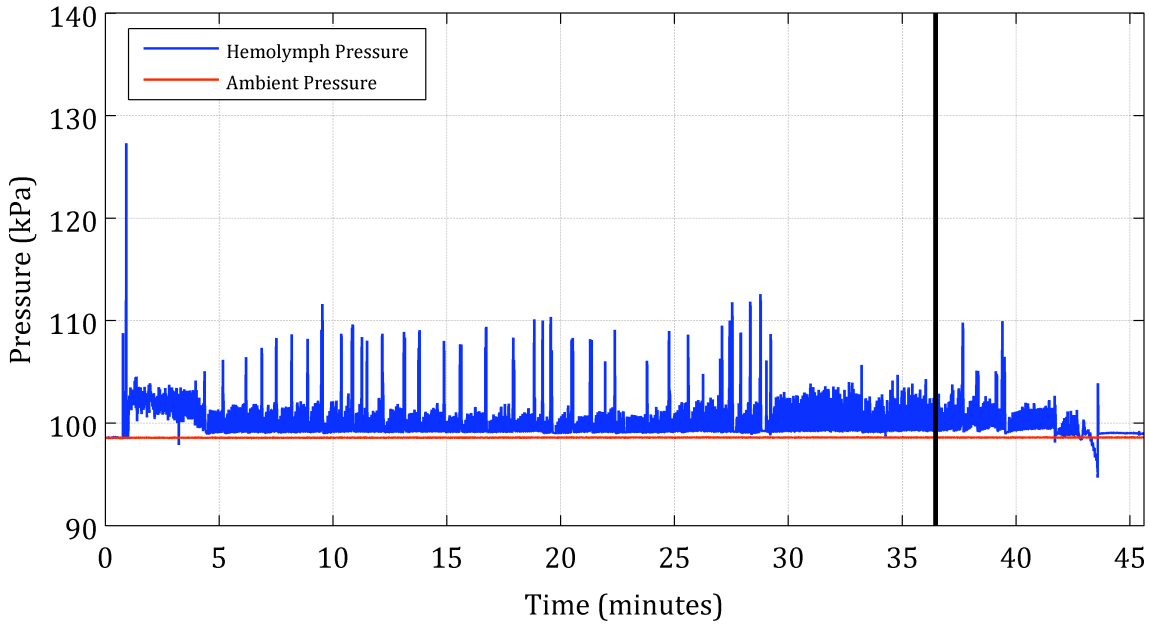

Figure B.1: Raw data associated with pressure trace in Figure 3.8a

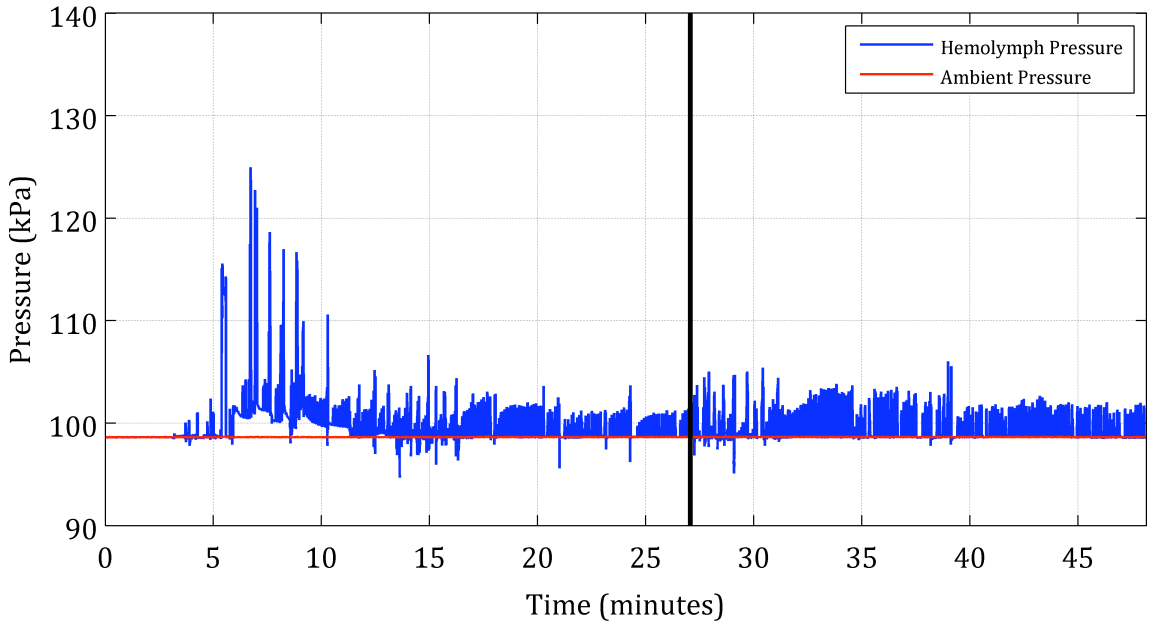

Figure B.2: Raw data associated with pressure trace in Figure 3.8b

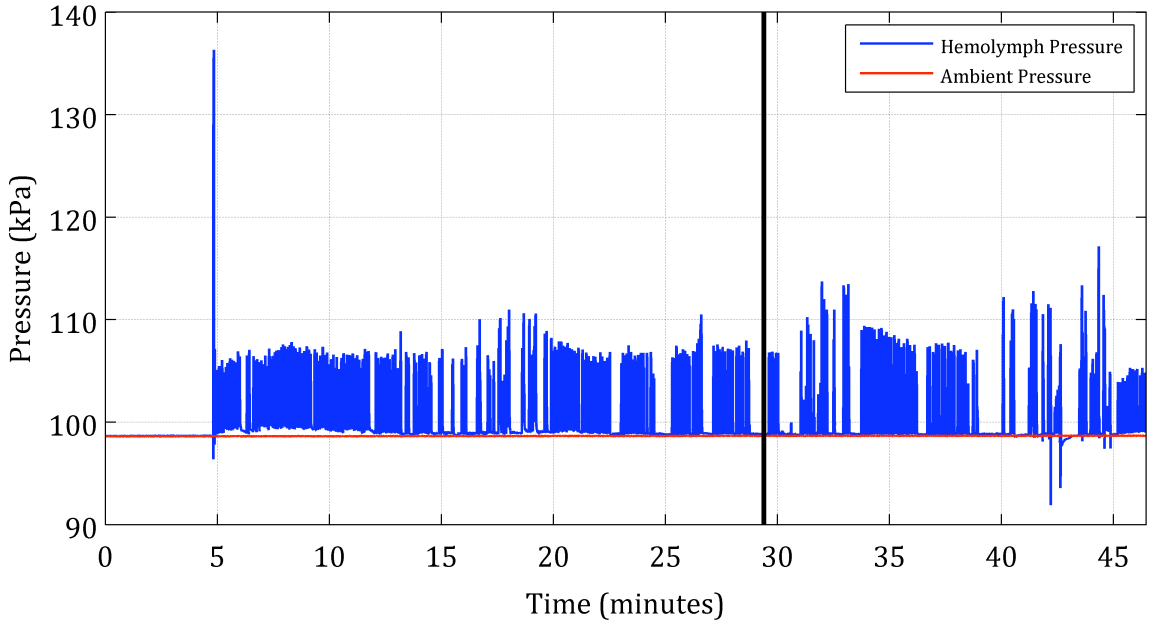

Figure B.3: Raw data associated with pressure trace in Figure 3.8c

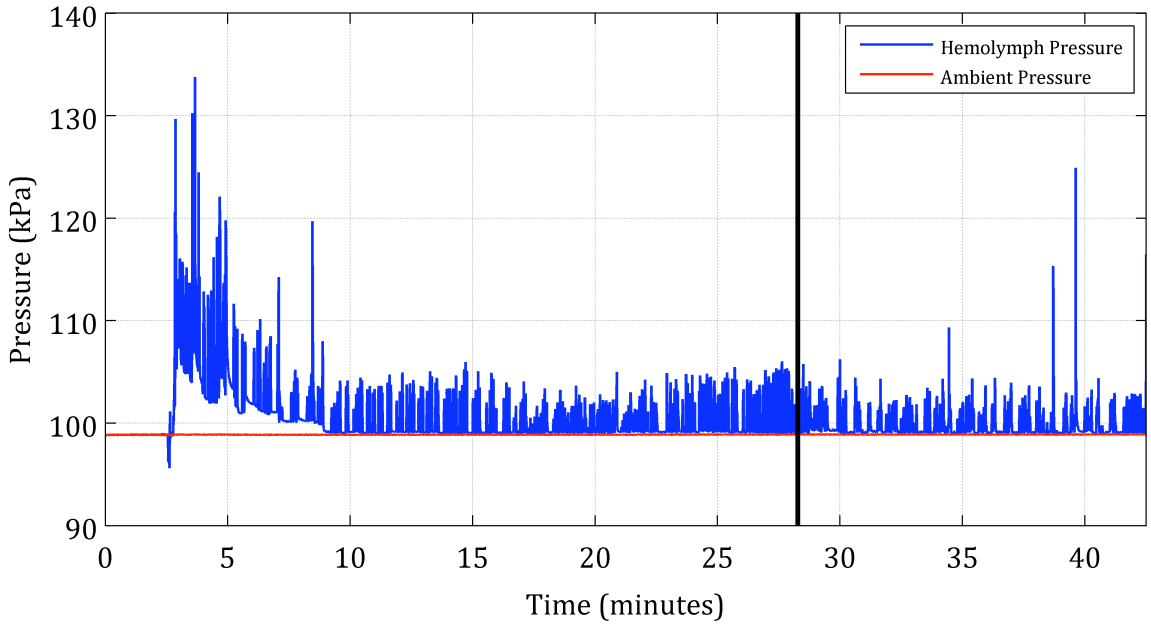

Figure B.4: Raw data associated with pressure trace in Figure 3.8d

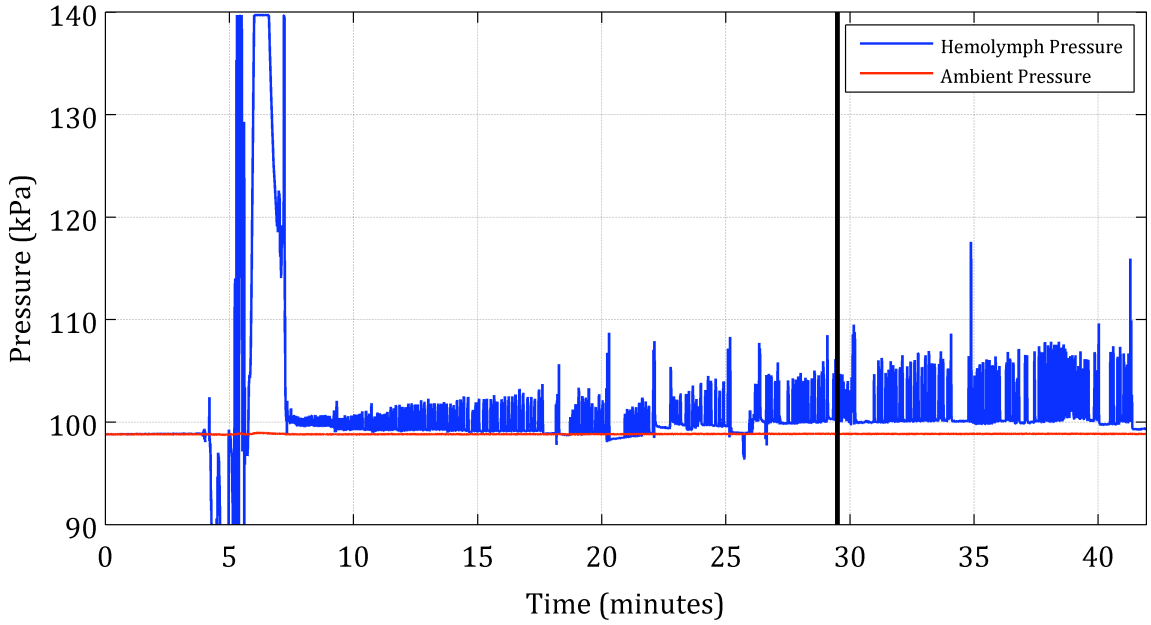

Figure B.5: Raw data associated with pressure trace in Figure 3.8e

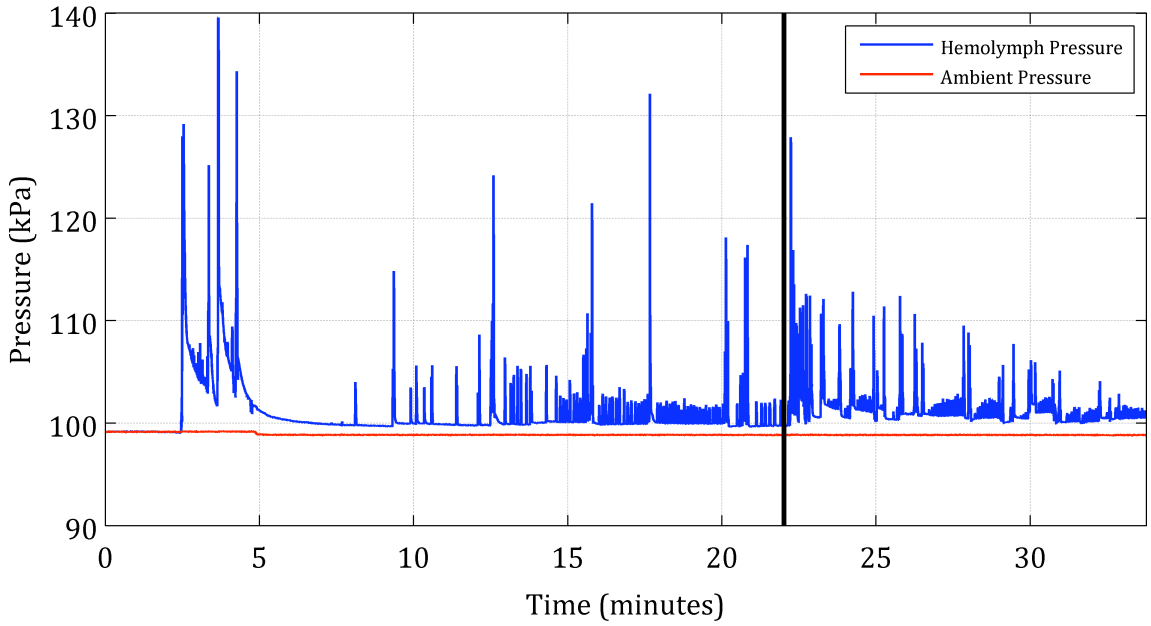

Figure B.6: Raw data associated with pressure trace in Figure 3.8f

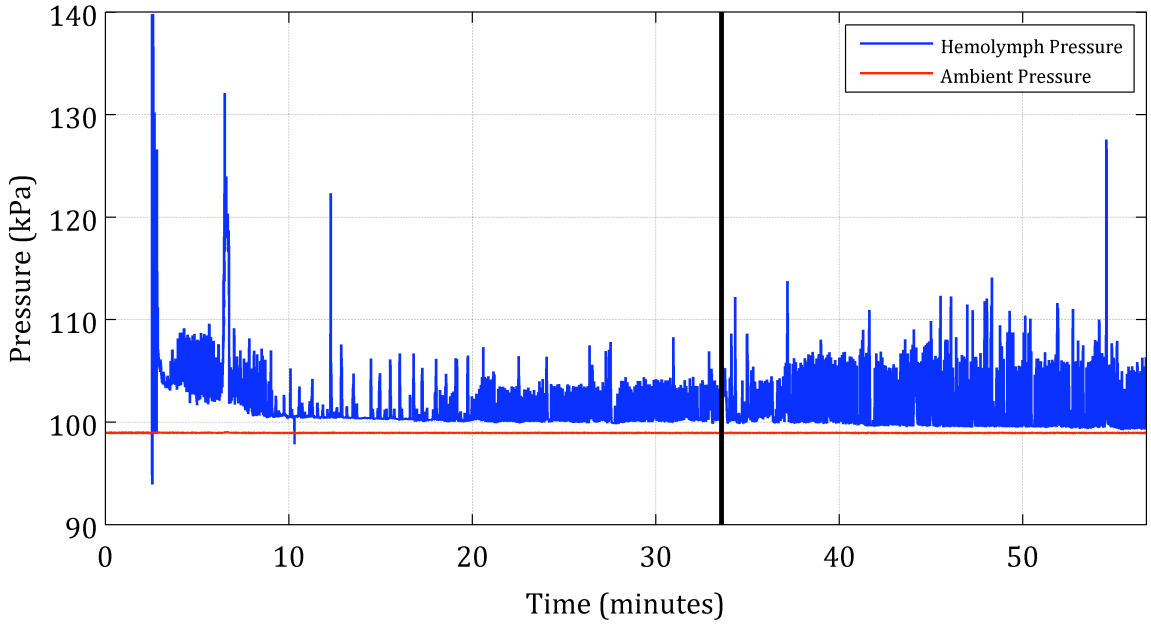

Figure B.7: Raw data associated with pressure trace in Figure 3.8g

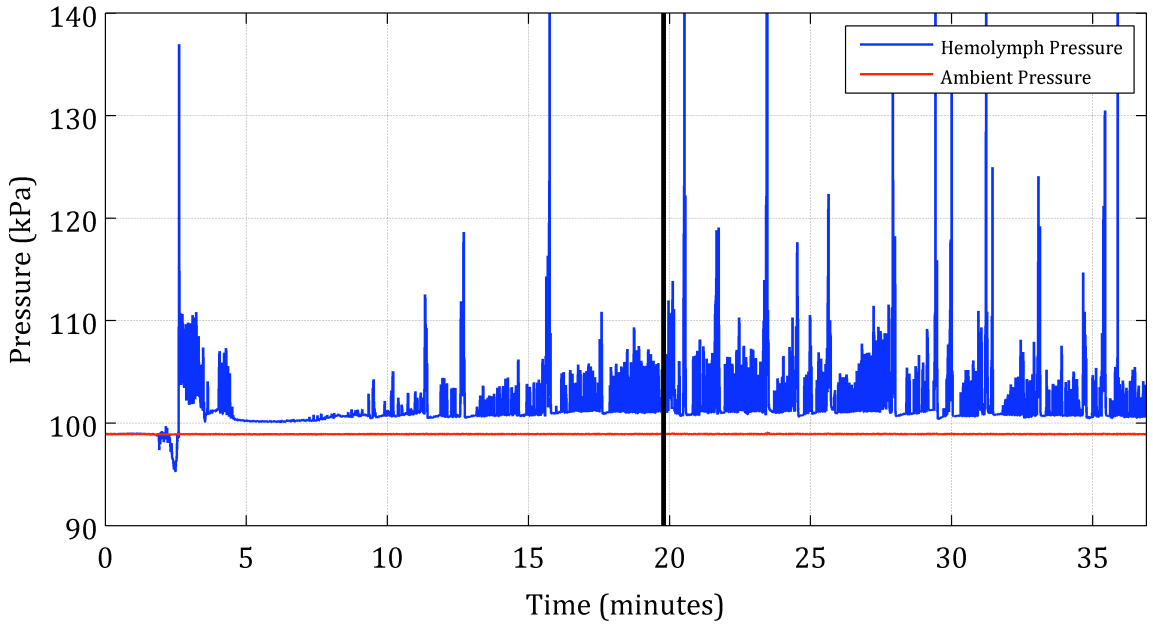

Figure B.8: Raw data associated with pressure trace in Figure 3.8h

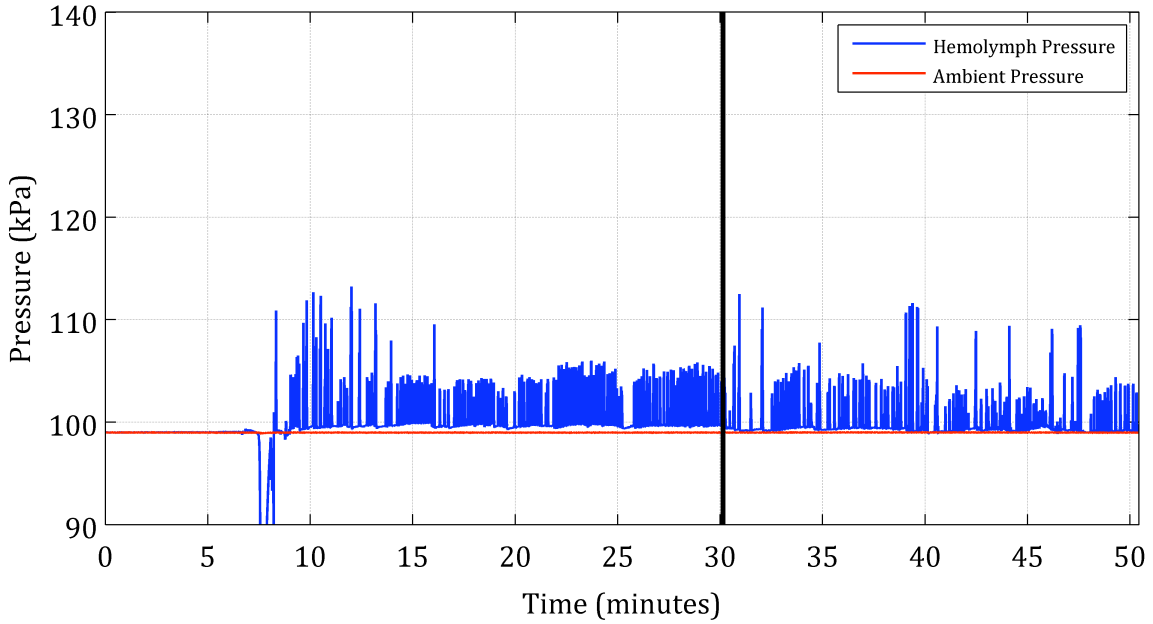

Figure B.9: Raw data associated with pressure trace in Figure 3.8i

Appendix C - Filtered Data Segments

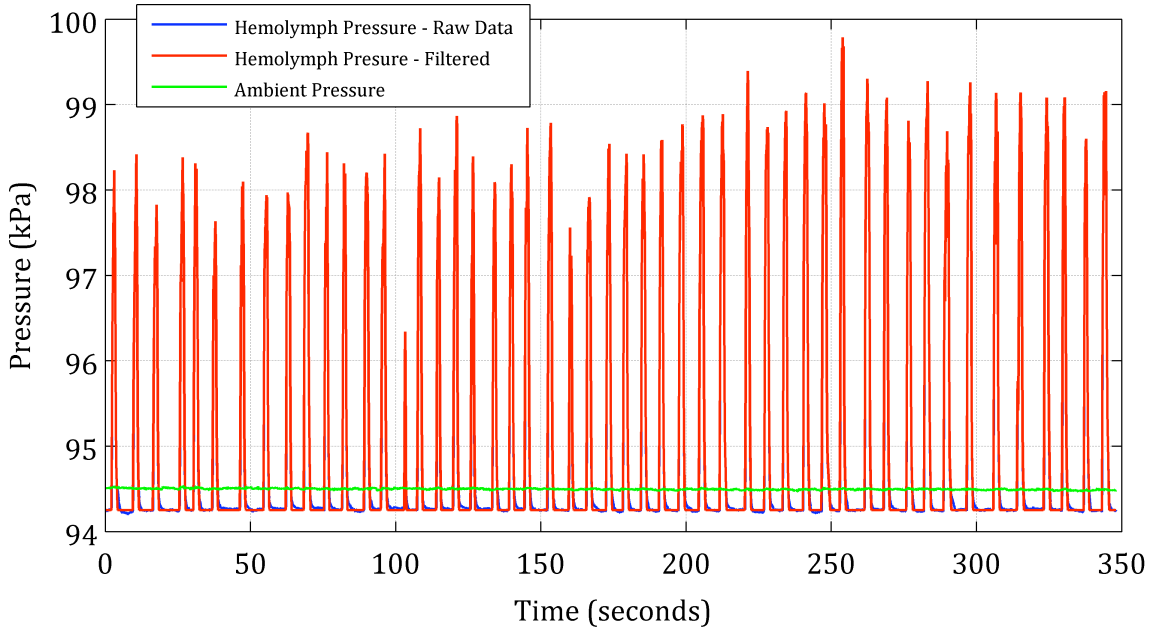

Figure C.1: Data sampled and filtered from the pressure trace in Figure 3.1a

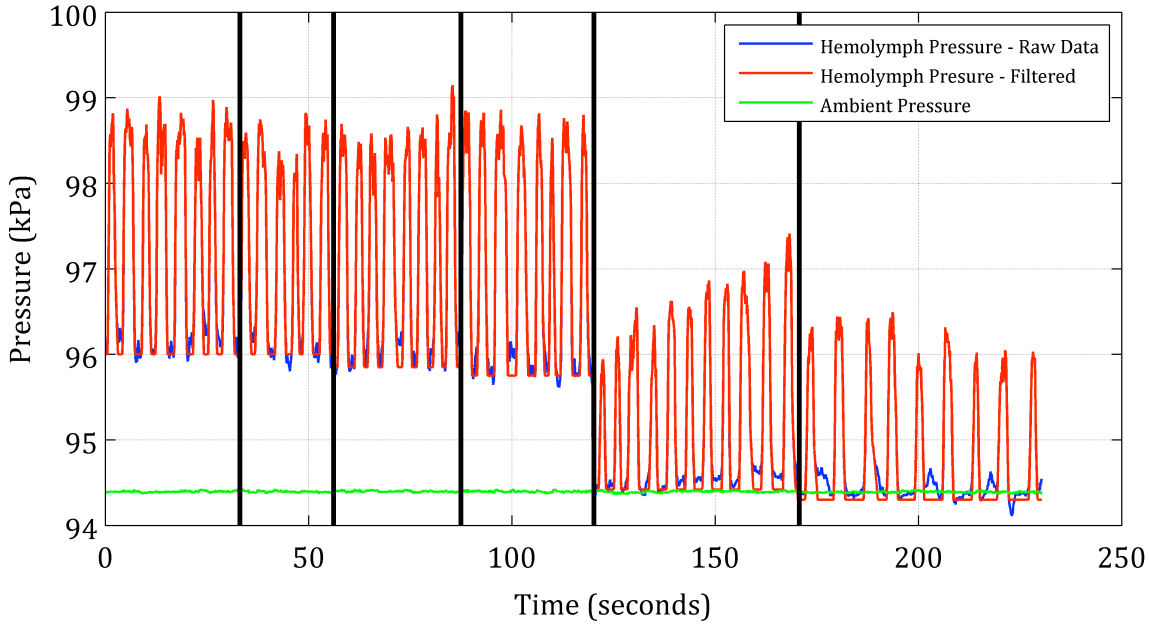

Figure C.2: Data sampled and filtered from the pressure trace in Figure 3.1b

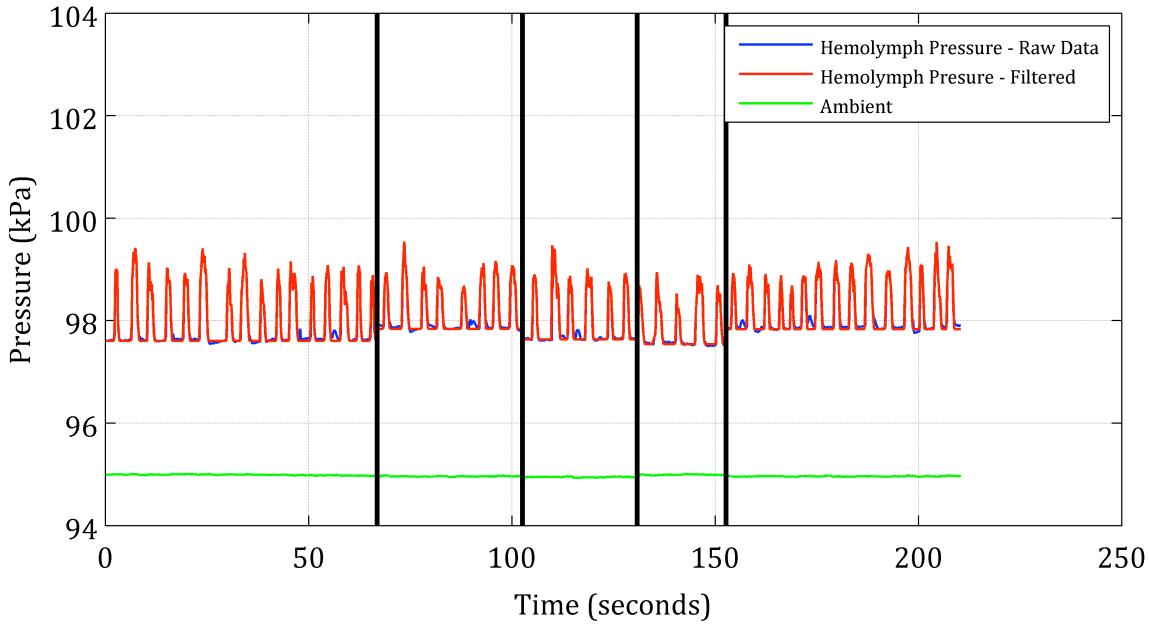

Figure C.3: Data sampled and filtered from the pressure trace in Figure 3.1c

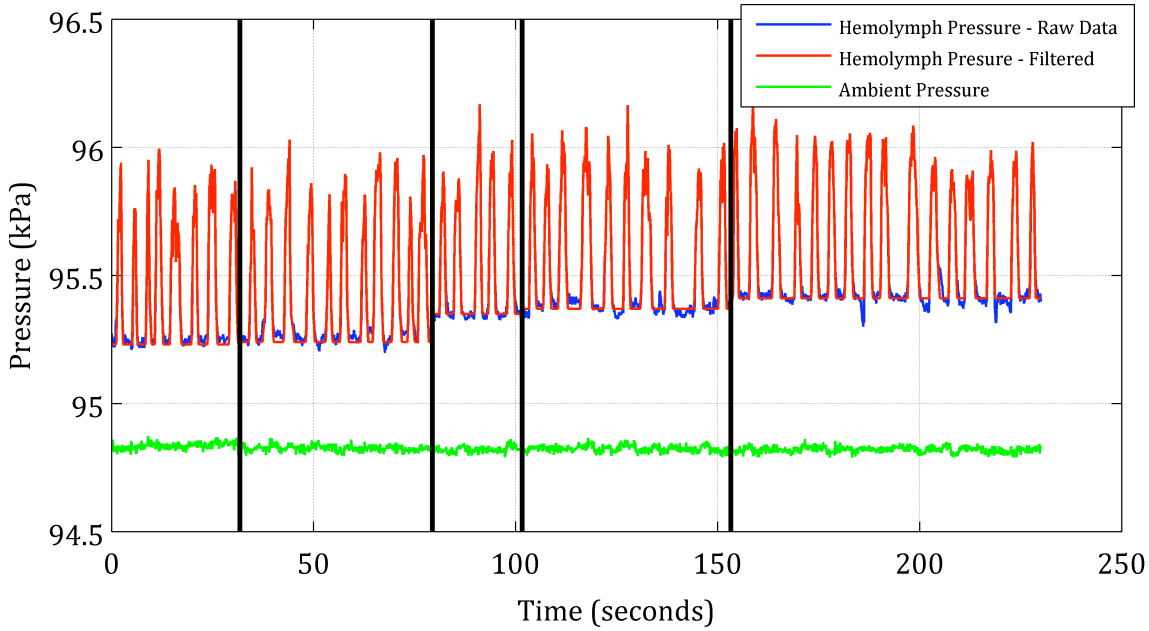

Figure C.4: Data sampled and filtered from the pressure trace in Figure 3.1d

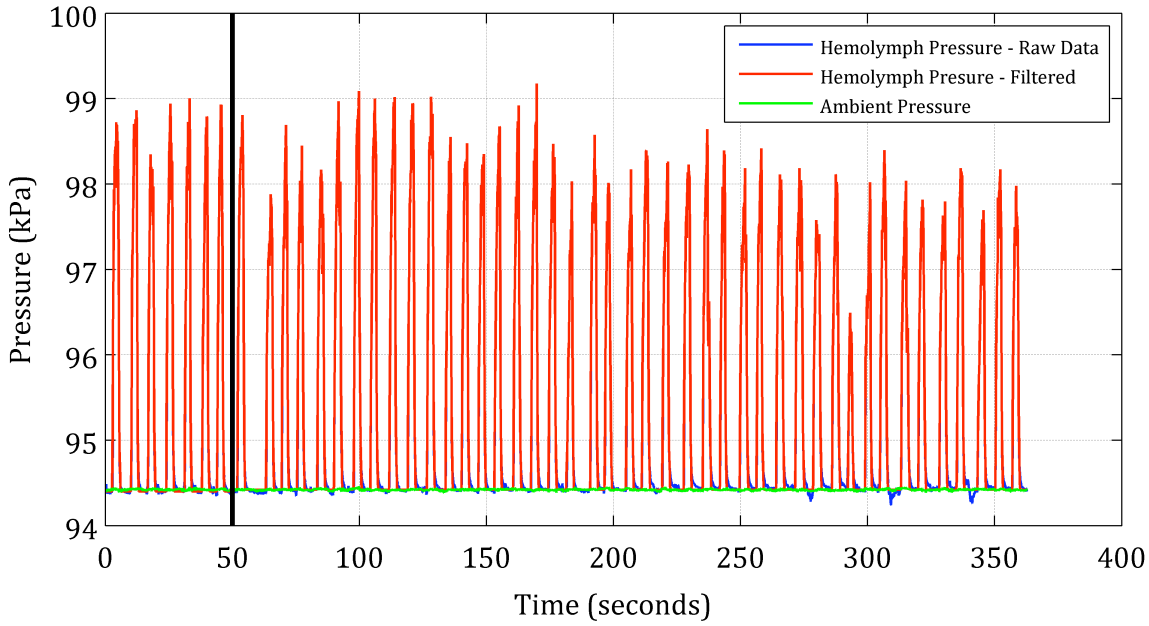

Figure C.5: Data sampled and filtered from the pressure trace in Figure 3.1e

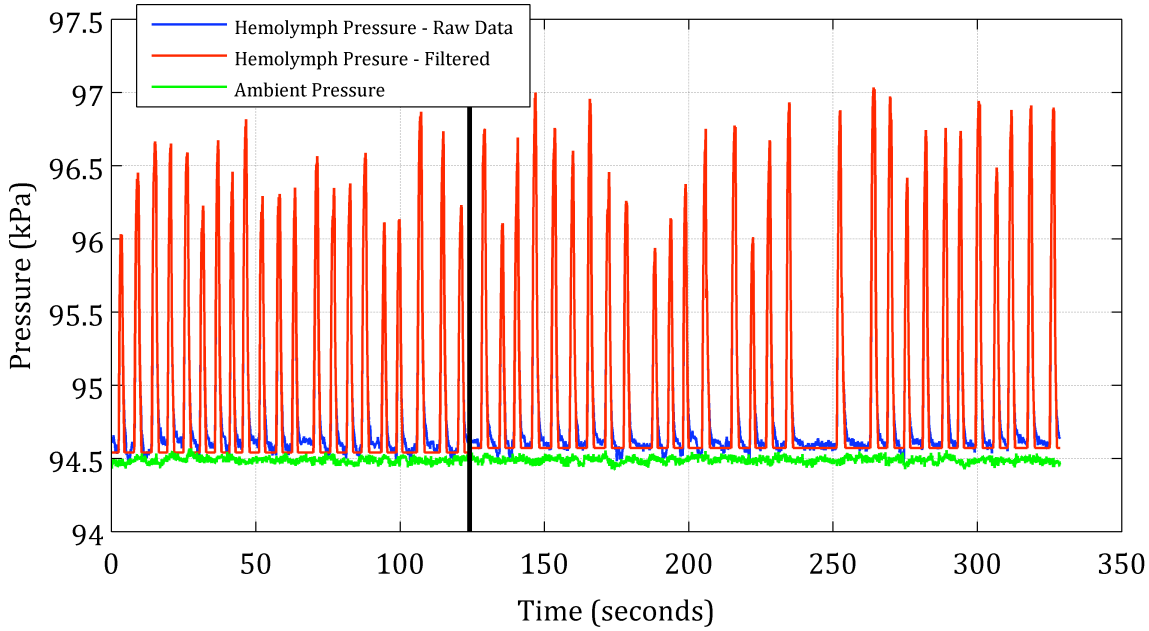

Figure C.6: Data sampled and filtered from the pressure trace in Figure 3.1f

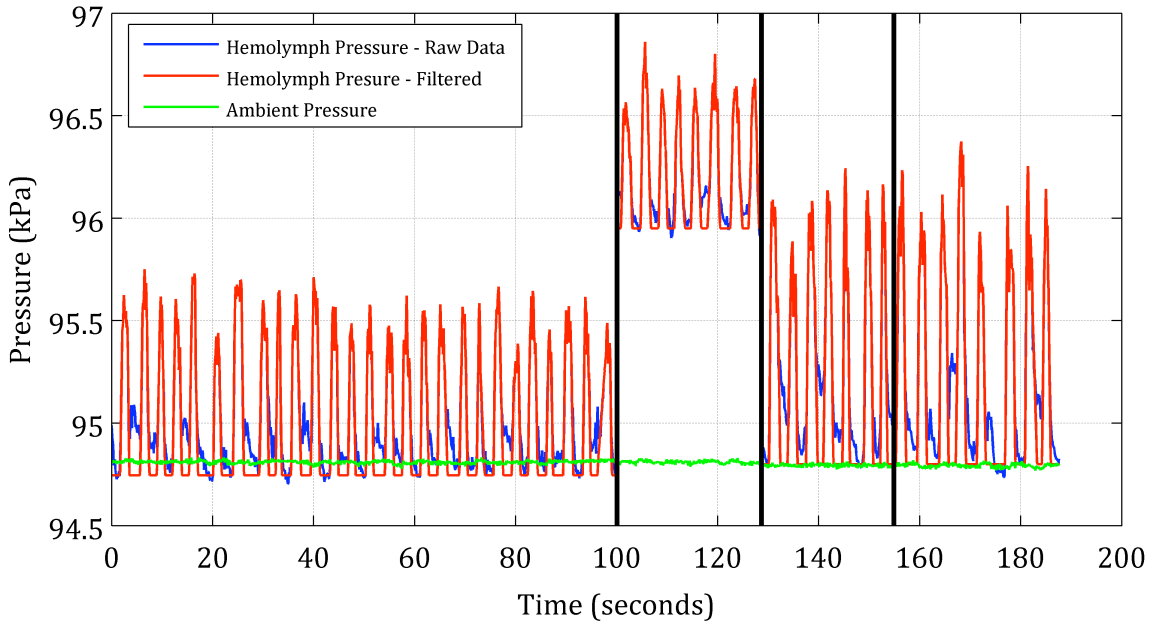

Figure C.7: Data sampled and filtered from the pressure trace in Figure 3.1g

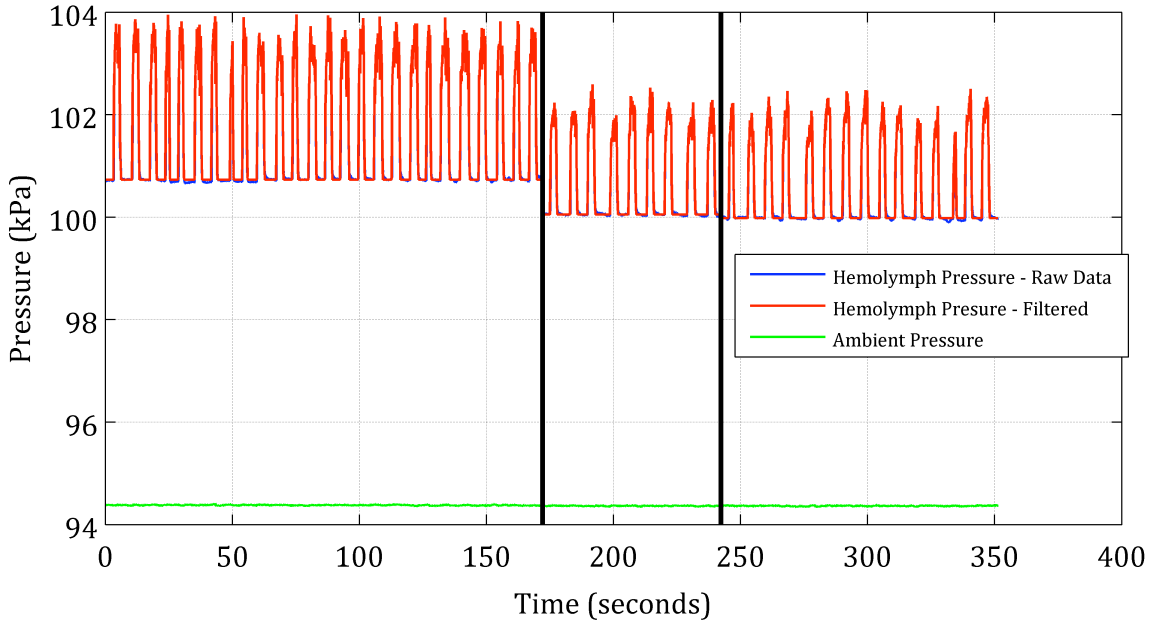

Figure C.8: Data sampled and filtered from the pressure trace in Figure 3.1h